

1 **Tectono-stratigraphy, formation and emplacement ages of the Beyşehir-Hoyran Nappes**
2 **in the south of the Sultan Dağları (Isparta, SW Türkiye)**

3 **Ali ERGEN^a, Alper BOZKURT^a, Ercan TUNCA^a, Ayhan ILGAR^a, Aynur HAKYEMEZ^a**

4 *^aGeneral Directorate of Mineral Research and Exploration, Department of Geological Research, 06800,*
5 *Ankara, Türkiye. 0000-0003-3740-9638, 0000-0001-5515-5577, 0000-0003-3230-2575, 0000-0002-5185-9697,*
6 *0000-0003-2470-1496 (www.orcid.org)*

7
8 **Corresponding author: Ali ERGEN, ali.ergen@mta.gov.tr*

9
10 **ABSTRACT**

11 The Beyşehir-Hoyran Nappes (BHN), in the south of Sultan Dağları, consist of ophiolite, mélangé and nappe
12 slices of different lithologies and ages belonging to the oceanic crust and related rocks, which originated from
13 the northern Neotethys and were thrust southwards over the Taurus Platform. These nappes, namely the
14 Marmaris ophiolite nappe, the Gülbahar nappe and the Domuzdağ nappe, are represented by three tectonically
15 related nappe-slices that extend as a narrow NW-SE trending belt to the south of the Sultan Dağları. The
16 Marmaris ophiolite nappe (Upper Cretaceous) is formed by three subunits namely the Marmaris ophiolite, the
17 Kızılcadağ mélangé and the Yenicekale metamorphics. Hornblende minerals from amphibolites of the
18 Yenicekale metamorphic rock unit yielded a ⁴⁰Ar-³⁹Ar age of 93.9±0.34 Ma (Cenomanian-Turonian boundary).
19 Besides, late Triassic to early Jurassic ages were obtained from the deep marine sedimentary rocks of the
20 Gülbahar nappe based on the radiolarian assemblages.

21 Paleontological and radiometric ages obtained from this study show that the formation of the BHN should
22 began in the Turonian and ended in the Late Maastrichtian. The nappes, on the other hand, were emplaced over
23 southern Sultan Dağları in the early-middle Paleocene and reached their present position as a result of late
24 Eocene movements.

25 **Key words:** Beyşehir-Hoyran nappes, Sultan Dağları, Gülbahar nappe, Metamorphic sole.

26
27 **1. Introduction**

28 Türkiye, which is situated on the Alpine-Himalayan orogenic belt, has been significantly shaped by the
29 closure of the Neotethys Ocean during the Late Cretaceous-Early Cenozoic and the subsequent collision between
30 the Anatolian and Arabian plates by the end of the Middle Miocene (Şengör and Yılmaz, 1981). During this
31 process, several suture zones developed in Türkiye. The İzmir-Ankara-Erzincan suture zone (Şengör and
32 Yılmaz, 1981; Görür et al., 1983; Okay and Tüysüz, 1999) and the Inner-Tauride suture zone (Görür et al., 1984;
33 Robertson and Dixon, 1984; Okay and Tüysüz, 1999), formed by the closure of the northern branch of the
34 Neotethys Ocean, constitutes the northern boundary of the Anatolide-Tauride Block (Okay and Tüysüz, 1999),
35 while the Bitlis-Zagros suture zone (Şengör and Yılmaz, 1981; Yılmaz, 1993; Parlak et al., 2009), formed by the
36 closure of the southern branch, defines the southern boundary.

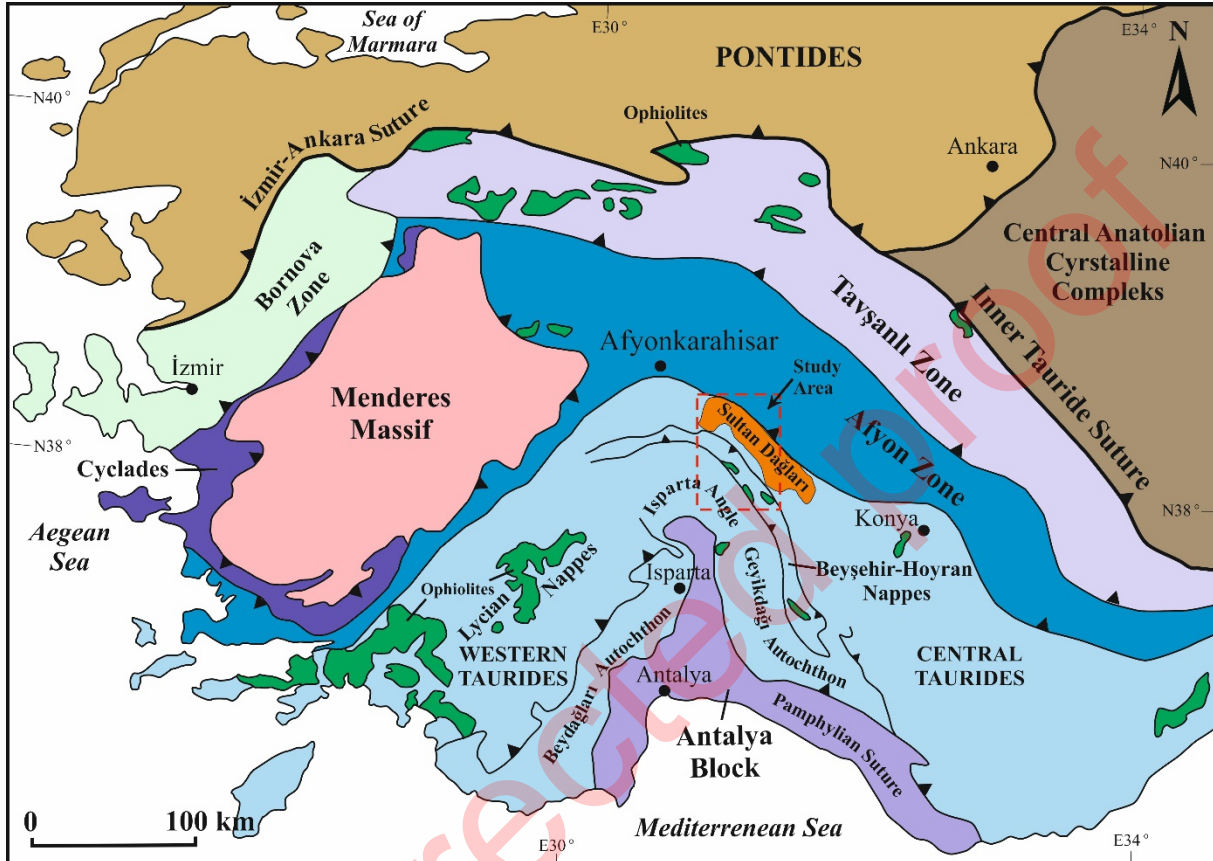
37 The Anatolides (*sensu* Ketin, 1966), located in the Anatolide-Tauride Block, represent those parts of the
38 Taurides that underwent regional metamorphism during the Late Cretaceous-Early Cenozoic due to the Alpine
39 orogeny (e.g., Pourceau et al., 2013). The Taurides consist mainly of parautochthonous and allochthonous,
40 imbricated, folded, non-metamorphic or low-grade metamorphic units (Geyikdağ, Aladağ, Bolkardağ, Bozkır,
41 Antalya and Alanya units) (Özgül, 1976). The Sultan Dağları and its surroundings is one of the regions where
42 the relationships between Geyikdağ, Aladağ and Bozkır units can be best observed.

43 The Sultan Dağları is a mountain range consisting of Paleozoic to Mesozoic low-grade metamorphic rocks
44 and a Cenozoic cover that extends between the Afyon Zone (Okay, 1984; Okay and Tüysüz, 1999; Candan et al.,
45 2005) and the Anamas-Akseki Autochthon (Şenel et al., 1992) with a NW-SE direction and forms the NE flank
46 of the Isparta Angle (*sensu* Poisson et al., 1984). The NW-SE trending allochthonous units extending south of the
47 Sultan Dağları are referred to as the BHN (Gutnic et al., 1968; Monod, 1977) (Figure 1). The BHN is composed
48 of ophiolites, mélanges and rocks of different ages and lithologies, derived from the northern branch of the
49 Neotethys Ocean (İzmir-Ankara-Erzincan and/or Inner Tauride Oceans) and emplaced on the Taurus platform
50 (Andrew and Robertson 2002; Çelik and Delaloye, 2006; Elitok and Drüppel, 2008). The BHN can be regarded
51 as the eastern continuation of the Lycian Nappes (*sensu* Şenel et al., 1989), which lies west of the Isparta Angle.

52 Units of the BHN are genetically represented in the northern branch of the Neotethys by rift-related rocks in
53 the Triassic, by carbonate and clastic sediments of the passive continental margin in the Jurassic-Cretaceous, and
54 by supra-subduction ophiolites and mélanges associated with northward subduction in the Late Cretaceous
55 (Andrew and Robertson, 2002; Çelik and Delaloye, 2006; Elitok and Drüppel, 2006; Mackintosh and Robertson,
56 2009; Parlak et al., 2019). The formation and emplacement processes of the BHN are key to understanding the
57 geodynamic evolution of the region. The general assumption about these nappes is that they were formed in the
58 Late Cretaceous due to the closure of the northern branch of the Neotethys and emplaced on the Taurus platform
59 during the Late Cretaceous-Eocene interval (Andrew and Robertson, 2002; Çelik and Delaloye, 2006; Elitok and
60 Drüppel, 2008; Güngör, 2013). Constraining these too-long intervals by paleontological and radiometric dating
61 provides more accurate data on the formation and emplacement processes of the BHN. In addition, the majority
62 of present studies of the BHN are concerned with the age and geochemical properties of the ophiolites and
63 metamorphic sole rocks (e.g. Elitok and Drüppel, 2002; Çelik and Delaloye, 2006; Parlak et al., 2019). Thus, the
64 tectono-stratigraphy of the nappes and their relationship to the cover rocks has not been sufficiently investigated.

65 This study aims to provide a detailed tectono-stratigraphy of the BHN and to constrain the formation and
66 emplacement ages of these nappes by integrating the biostratigraphic, radiometric and structural data.

67



68

69 Figure 1- Tectonic map of the western Anatolia (modified after Pourteau et al., 2010, 2013).

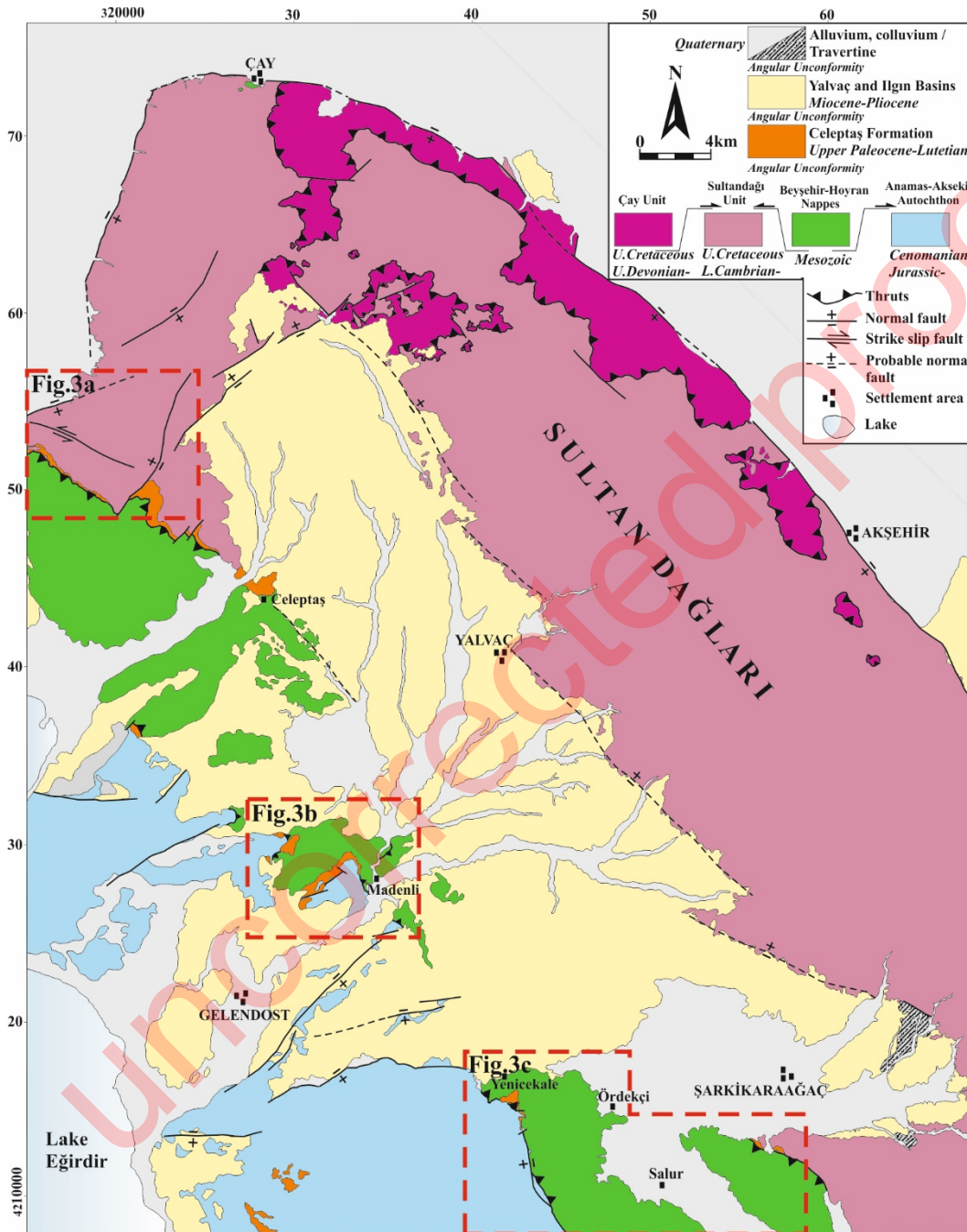
70

71 1.1. Material and Method

72 Basic studies to identify tectono-stratigraphic features and solve geological problems are based on the
73 production of geological maps at a scale of 1:25,000 in the field. The paleontological and petrographic samples
74 studied in the MTA laboratories were collected in the field from appropriate levels of the formations.
75 Radiometric dating studies were carried out at the Nevada Isotope Geochronology Laboratory (USA) using the
76 ^{40}Ar - ^{39}Ar method on hornblende minerals from amphibolites of the Yenicekale metamorphics.

77 2. Tectono-stratigraphy

78 Early Cambrian to Quaternary rock units of different origins and lithologies outcrop in the study area (Figure
 79 2). Formations of the Geyikdağı, Bolkardağı/Aladağ and Bozkır units form the basement of the region (Özgül,
 80 1976).
 81

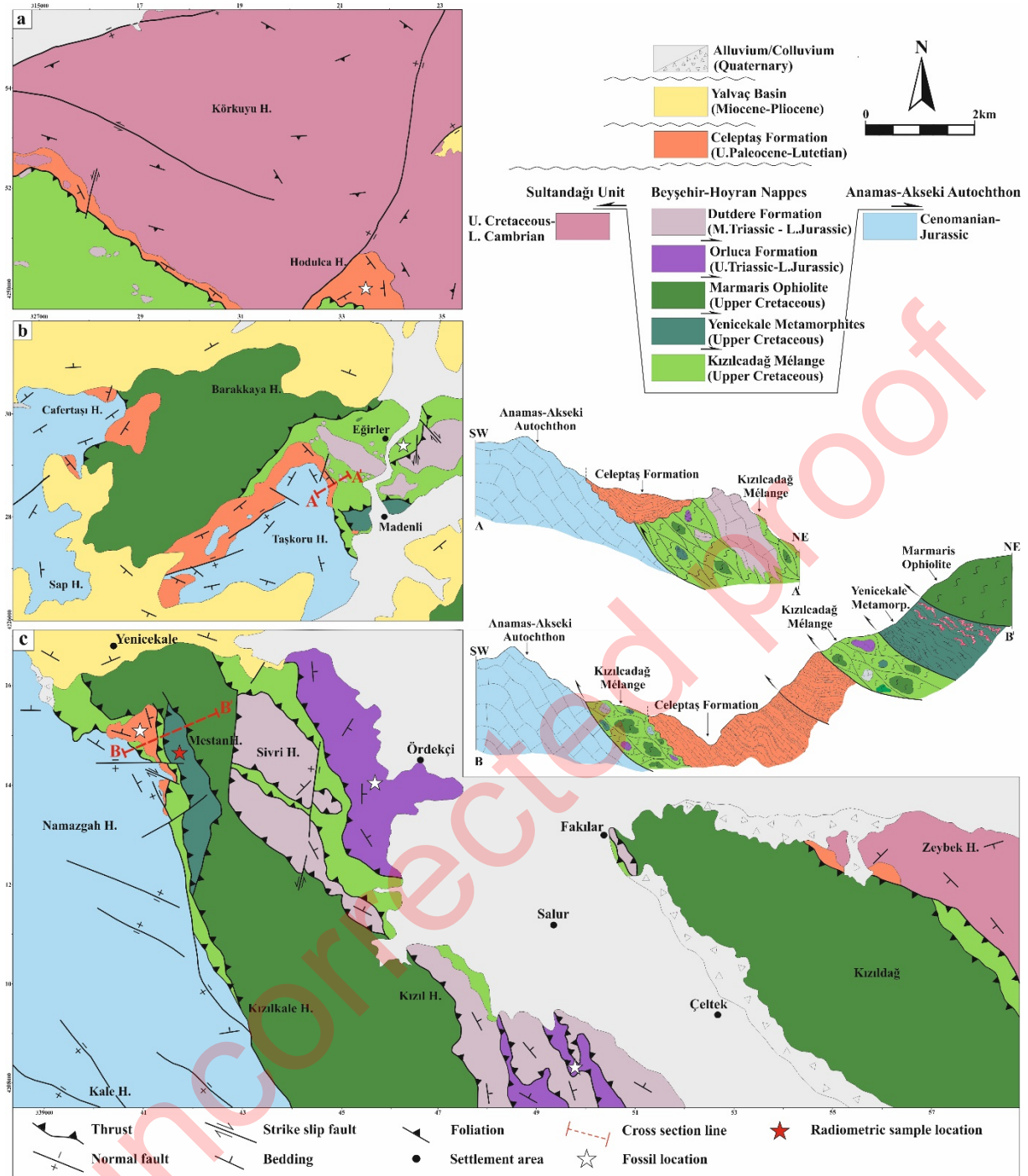


82
 83 Figure 2- Simplified geological map of the Sultan Dağları and its surroundings (simplified after Ergen et al.,
 84 2021).
 85

86 The widespread parautochthonous rocks of the Geyikdağı Unit (Özgül, 1976) are studied under the names of
87 Sultandağı Unit (*sensu* Özgül et al., 1991) and Anamas-Akseki Autochthon (*sensu* Şenel et al., 1992) in the
88 study area, while the allochthonous rock assemblages of the Bolkardağı/Aladağ Unit and the Bozkır Unit are
89 studied under the names of Çay Unit (*sensu* Özgül et al., 1991) and the BHN (*sensu* Monod, 1977) respectively
90 (Figures 2 and 3).

91 The late Paleocene-Lutetian Celeptaş Formation and deposits of the Miocene-Pliocene Yalvaç and Iğın
92 basins form the Cenozoic cover. Quaternary deposits are the youngest cover in the region. As the units of the
93 BHN observed in the study area are a continuation of the Lycian Nappes and show strong stratigraphic
94 similarities, the nomenclature of the Lycian Nappes is followed to ensure regional correlation.

95



96

97 Figure 3- Geological map and cross-sections showing the relationship of the units of the BHN to the
 98 parautochthonous basement and cover rocks (modified after Ergen et al., 2021).

99

100 2.1. Sultandağı Unit

101 The Sultandağı Unit forms the dominant rock mass of the Sultan Dağları. The unit consists of lower
 102 Cambrian to Upper Cretaceous metasedimentary and metavolcanic rocks (Özgül et al., 1991; Ergen et al., 2021).

103 The Sultandağı Unit, which represents a transgressive sequence associated with back-arc basin development in
104 the early Paleozoic (Linneman et al., 2008; Nance et al., 2010; Dedeoğlu et al., 2021), is composed of quartzite,
105 marble and turbiditic clastic rocks. An upper Paleozoic succession of quartzite, phyllite, recrystallized limestone
106 and dolomite overlies the early Paleozoic units after the Late Devonian unconformity. The Mesozoic succession
107 begins in the Middle Triassic with terrestrial metaconglomerates and metasandstones, overlain by Jurassic-
108 Cretaceous metacarbonate rocks. The Sultandağı Unit underwent lower greenschist metamorphism (Güngör,
109 2013) in the early-middle Paleocene based on the emplacement of the Çay Unit and the BHN (Ergen et al., 2021;
110 Ergen, 2023). The late Paleocene-Lutetian Celeptaş Formation and the Neogene deposits of the Yalvaç and Ilgın
111 basins unconformably overlie the Sultandağı Unit.

112 2.2. Anamas-Akseki Autochthon

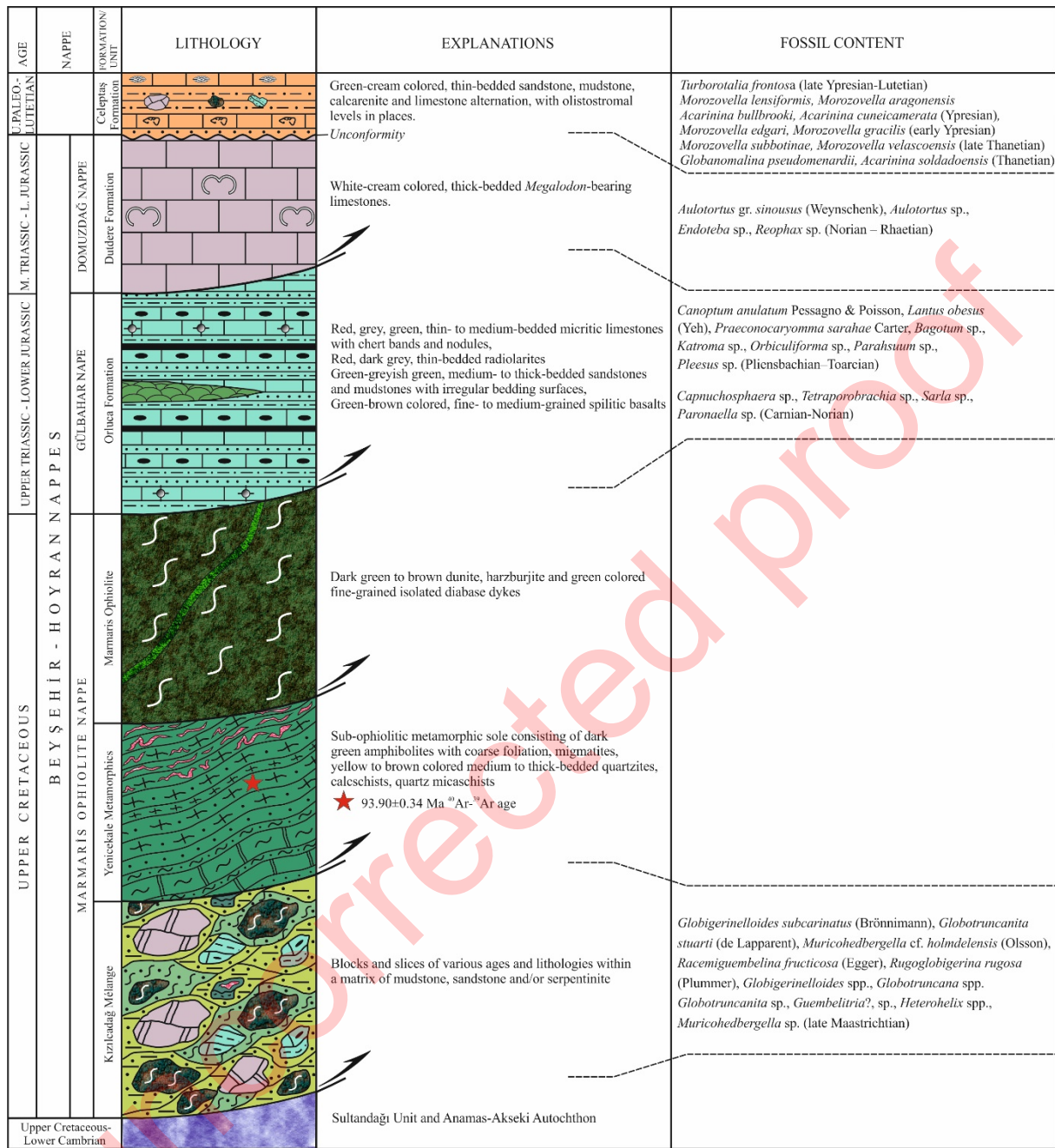
113 The unit consists of non-metamorphic Jurassic-Cretaceous aged (Şenel et al., 1992) neritic carbonates
114 belonging to the Geyikdağı Unit in the south of the Sultan Dağları. The Anamas-Akseki Autochthon (*sensu*
115 Şenel et al., 1992), observed in the SW parts of the study area, is represented by Jurassic-Cenomanian grey-
116 colored, medium to thick-bedded limestones and dolomites. The lower contact of the unit is not seen in the study
117 area, being unconformably overlain by the Celeptaş Formation and tectonically overlain in places by ophiolites
118 of the BHN.

119 2.3. Çay Unit

120 The Late Devonian to Cretaceous lower greenschist-facies rocks of the Bolkardağı/Aladağ Unit, outcropping
121 in a NW-SE trending narrow strip along the northeastern edge of the Sultan Dağları, are called the Çay Unit
122 (Özgül et al., 1991; Ergen et al., 2021). The Çay Unit, which consists of metasedimentary rocks intercalated with
123 metavolcanics, tectonically overlies the Sultandağı Unit and is also tectonically overlain by the BHN (Figure 2).

124 2.4. Beyşehir-Hoyran Nappes

125 The BHN are the allocthonous masses composed of ophiolite, mélange and associated blocks and slices of
126 different lithologies and ages, formed as a result of the closure of the northern branch of the Neotethys Ocean
127 and were emplaced on the Taurus Platform during the Late Cretaceous-early Cenozoic (Monod, 1977; Andrew
128 and Robertson, 2002; Çelik and Delaloye, 2006; Ergen et al., 2021). These nappes, which are exposed in a NW-
129 SE trending narrow belt and are tectonically interrelated with each other, are the Marmaris Ophiolite nappe (the
130 Kızılcadağ mélange, the Yenice kale metamorphics and the Marmaris ophiolite), the Gülbahar nappe and the
131 Domuzdağ nappe from bottom to top (Ergen et al., 2021; Ergen, 2023) (Figure 4).



133

134 Figure 4- Tectono-stratigraphic column of the BHN in the study area (not to scale).

135

136 The Marmaris ophiolite nappe (Upper Cretaceous) is formed by three subunits as the Marmaris ophiolite, the
 137 Kızılcaadağ mélangé and the Yenicekale metamorphics. The Marmaris ophiolite is composed of dunitic,
 138 harzburgite, serpentinite and diabase dykes, while the Kızılcaadağ mélangé is composed by blocks of different
 139 ages and lithologies contained in an ophiolitic/sedimentary matrix. The Yenicekale metamorphics consist mainly

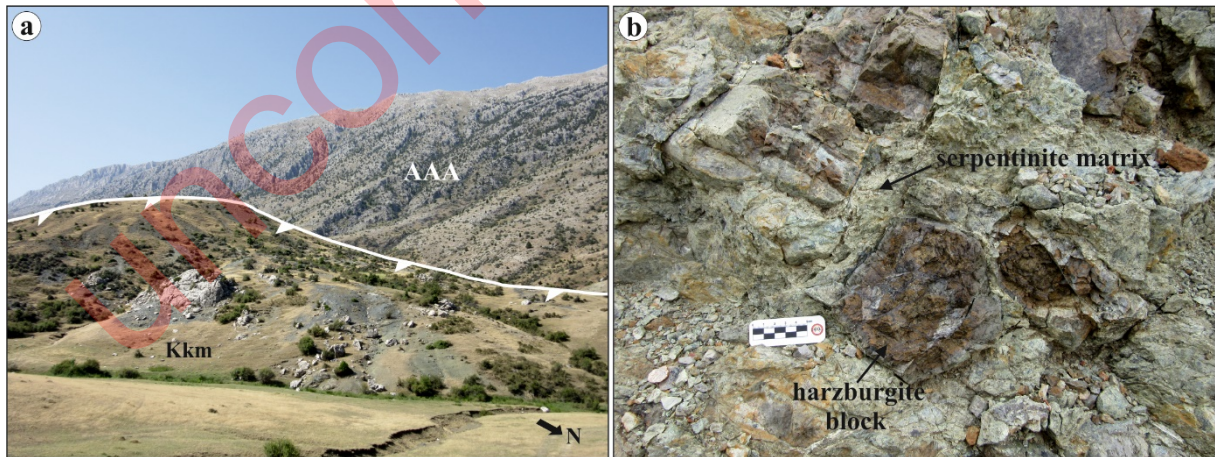
140 of amphibolites that characterize a sub-ophiolitic metamorphic sole (Elitok and Drüppel, 2008). The Orluca
141 Formation (Şenel et al., 1989), which is composed of micritic limestone, radiolarite, chert, mudstone and basalt
142 intercalations, represents the Gülbahar nappe. The Domuzdağ nappe at the top is represented by the Dutdere
143 Formation (Ersoy, 1989), which consists of *Megalodon*-bearing limestones.

144 The Celeptaş Formation unconformably overlies the BHN, which tectonically rest on the parautochthonous
145 Sultandağı Unit and the Anamas-Akseki Autochthon.

146 2.4.1. Marmaris Ophiolite Nappe

147 *Kızıladağ mélange (Kkm)*: It is composed of blocks and slices of different lithologies contained in an ophiolitic
148 and sedimentary matrix (Poison, 1977; Şenel et al., 1989; Ergen et al., 2021). The majority of the matrix consists
149 of green, intensely sheared serpentinites and, to a lesser extent, mudstones. Blocks and slices belonging to the
150 Domuzdağ and Gülbahar nappes and the Marmaris Ophiolite are observed in the matrix. Blocks and slices of the
151 Domuzdağ and Gülbahar nappes and the Marmaris Ophiolite, ranging from a few centimetres to tens of metres,
152 are observed in the matrix, and they are composed of such rocks as marble, micritic limestone, chert, radiolarite,
153 dunite, harzburgite, gabbro, diabase and amphibolite (Figures 5a and 5b). Radiolarian assemblages obtained
154 from micritic limestone, chert and radiolarite blocks of the formation yielded ages from Aalenian to early
155 Tithonian.

156



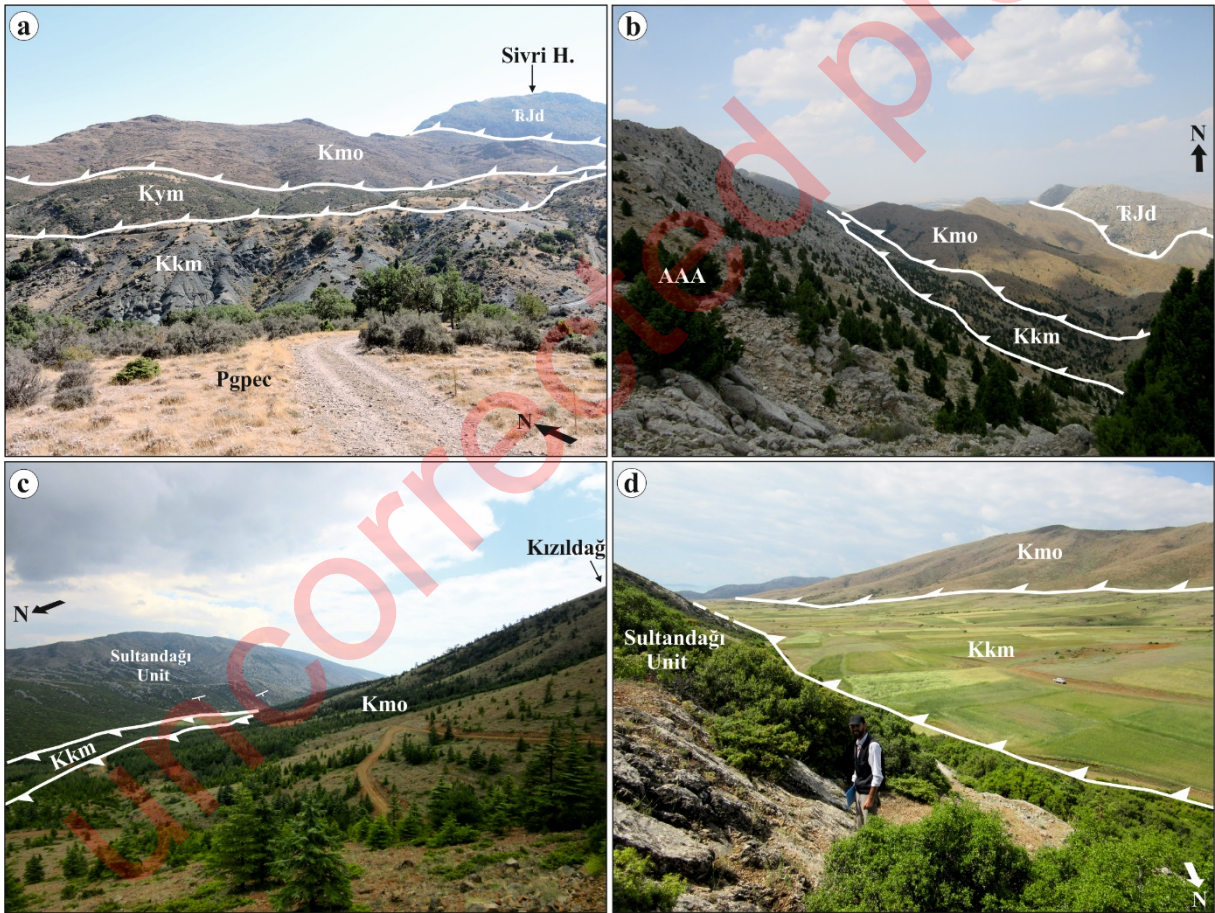
157

158 Figure 5- a) General view of the Kızıladağ mélange (Kkm) and its tectonic contact with the Anamas-Akseki
159 Autochthon (AAA), b) harzburgite blocks in the serpentinite matrix of the mélange, south of
160 Yenice kale village, Şarkikarağaç.

161

162 The lower contact of the Kızıladağ mélangé is tectonic. It tectonically overlies the Jurassic-Cretaceous
163 carbonates of the Sultandağı Unit to the south of Şarkikaraağaç, while tectonically overlying the Jurassic-
164 Cenomanian limestones of the Anamas-Akseki Autochthon to the south of Yenicekale (Figures 5a and 6a-d).
165 The Celeptaş Formation covers the Kızıladağ mélangé with an unconformable contact. In addition, the
166 Marmaris ophiolite, Yenicekale metamorphics, Domuzdağ and Gülbahar nappes tectonically overlie the
167 Kızıladağ mélangé. It is also unconformably overlain by deposits of the Miocene-Pliocene Yalvaç Basin to the
168 south of Yenicekale village (Figure 3c).

169



170

171 Figure 6- Tectonic relationships of units of the BHN. a, b) SW-vergent thrust contacts, SE of Yenicekale,
172 Şarkikaraağaç, c, d) NE-vergent back-thrusts, S of Şarkikaraağaç. Kmo: Marmaris ophiolite, Kkm:
173 Kızıladağ mélangé, Kym: Yenicekale metamorphics, TrJd: Dutdere Formation, AAA: Anamas-
174 Akseki Autochthon.

175

176 The age of the mélange in the Lycian Nappes is accepted as Late Cretaceous based on the planktonic
177 foraminiferal assemblages (Poisson, 1977; Şenel et al., 1989). Besides, it is claimed that the age of the mélange
178 near Bozkır town (Konya) is late Maastrichtian. It was also reported that the age of the mélange near Bozkır
179 district (Konya) is late Maastrichtian (Özgül, 1997; Andrew and Robertson, 2002).

180 In this current study, planktonic foraminiferal assemblage including *Globigerinelloides subcarinatus*
181 (Brönnimann), *Globotruncanita stuarti* (de Lapparent), *Muricohedbergella* cf. *holmdelensis* (Olsson),
182 *Racemiguembelina fructicosa* (Egger), *Rugoglobigerina rugosa* (Plummer), *Globigerinelloides* spp.,
183 *Globotruncana* spp. *Globotruncanita* sp., *Guembelitra*?, sp., *Heterohelix* spp., *Muricohedbergella* sp. species,
184 indicating a late Maastrichtian age, has been identified from the mudstones that forms the sedimentary matrix of
185 the Kızılcaadağ mélange around the Eğirler village.

186 In addition, assemblages containing radiolarian species such as *Transhsuum brevicostatum* gr. (Ozoldova),
187 *Zhamoidellum* sp., *Tritrabs casmaliaensis* (Pessagno), *Homoeoparonaella* sp. cf. *H. argolidensis* Baumgartner,
188 *Emiluvia* sp., *Mirifusus* sp., *Pantanellium* sp., *Mirifusus guadalupensis* Pessagno, *Archaeospongoprimum* sp.,
189 *Podobursa* sp., *Transhsuum* sp., *Praewilliriedellum convexum* (Yao), *Saitoum* sp., *Hsuum* sp., *Eucyrtidiellum*
190 *unumaense* s.l. (Yao), *Praewilliriedellum convexum* (Yao), *Transhsuum maxwelli* gr. (Pessagno),
191 *Homoeoparonaella* (?) *pseudoewingi* (Baumgartner), *Tetraditryma* sp. cf. *T. pseudoplana* Baumgartner, *Saitoum*
192 sp., *Hsuum* sp., *Parahsuum* sp. are obtained in different samples of micritic limestones and radiolarites of the
193 mélange, yielding an Aalenian-early Tithonian age. The Kızılcaadağ mélange was formed by the emplacement of
194 blocks and slices of different lithologies and ages in an ophiolitic/sedimentary matrix during the Late Cretaceous
195 northward subduction of the northern branch of the Neotethys Ocean, and thus gained a chaotic structure
196 depending on intense tectonics.

197 *Yenicekale Metamorphics (Kym)*: The rock assemblage containing amphibolite, amphibole-biotite schist,
198 calcschist and quartz schist, which are observed as sub-ophiolitic metamorphic sole in the BHN (Elitok and
199 Drüpbel, 2008), are referred to as the Yenicekale metamorphics (Ergen et al., 2020, 2021).

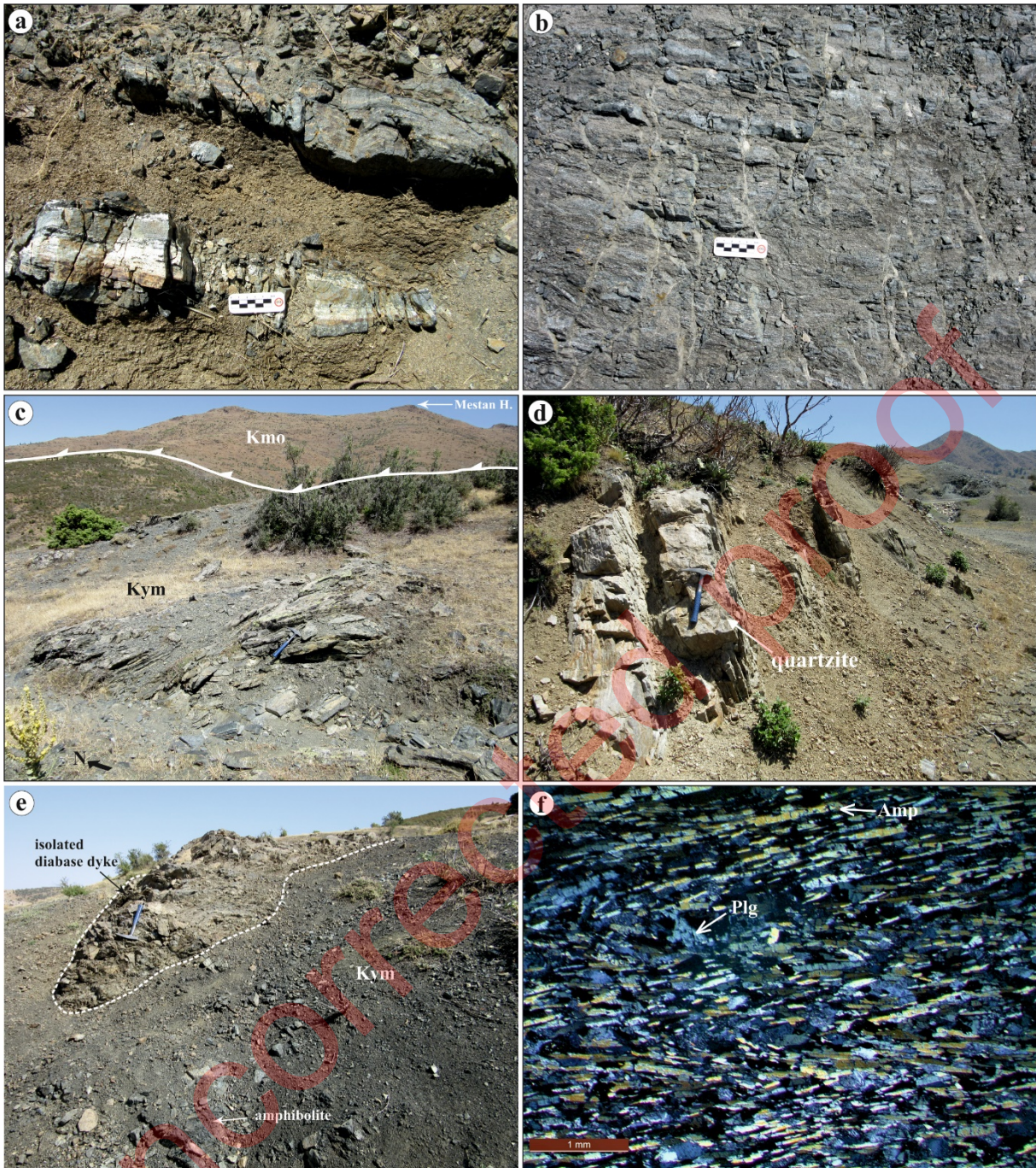
200 The Yenicekale metamorphics are composed of dark green, medium to coarsely foliated amphibolites, with
201 pygmatic folds in places (Figures 7a and 7b), and grey-blue, thin to medium-bedded calcschists and yellow-
202 brown, thin to medium foliated quartzites (Figure 7d) and quartz schists. Amphibolites, which are the dominant
203 lithologies of the unit, are composed of plagioclase, hornblende, chlorite and titanite minerals, with a

204 granonematoblastic to nematoblastic texture (Figure 7f). Sericitization and argillization are common in
205 plagioclase minerals. Quartzites are composed of quartz, feldspar, mica and apatite minerals, with a granoblastic
206 texture. These rocks show a metamorphic grade from amphibolite to greenschist facies (Elitok and Drüppel,
207 2008). Inverted metamorphic grade, one of the characteristic features of the sub-ophiolitic metamorphic rocks,
208 can be observed within the Yenicekale metamorphics. The amphibolites are at the top of the sequence, while the
209 greenschist facies rocks such as quartzite, quartz schist and calcschist are at the bottom of the sequence. These
210 metamorphic rocks are intruded by non-metamorphic isolated diabase dykes, as is in the Marmaris ophiolite
211 (Figure 7e). These dykes, which yield U-Pb zircon ages ranging from 90.8 ± 1.6 Ma to 87.6 ± 2.1 Ma (Parlak et
212 al., 2019), are geochemically tholeiitic and, to a lesser extent, alkaline in composition (Elitok and Drüppel, 2008;
213 Parlak et al., 2019).

214 The Yenicekale metamorphics are generally observed between the ophiolites and the ophiolitic mélange,
215 representing various thicknesses (Figure 6a-b and 7c). It has a thickness of up to 140 metres around Yenicekale
216 village (Elitok and Drüppel, 2008) and has a lenticular geometry.

217 Hornblende minerals from amphibolites of this unit in the south of Yenicekale village (coordinates:
218 36342124N/4214144E) yielded a ^{40}Ar - ^{39}Ar age of 93.90 ± 0.34 Ma (Figure 8). Parlak et al. (2019) obtained ages
219 of 90-94 Ma and 91-93 Ma from amphibolites in the same area using U-Pb and ^{40}Ar - ^{39}Ar methods, respectively.
220 These are in agreement with the 91-93 Ma age of Çelik et al. (2006) determined from amphibole and mica
221 minerals of the Lycian Nappes, Antalya Nappes and metamorphic basement rocks of the BHN.

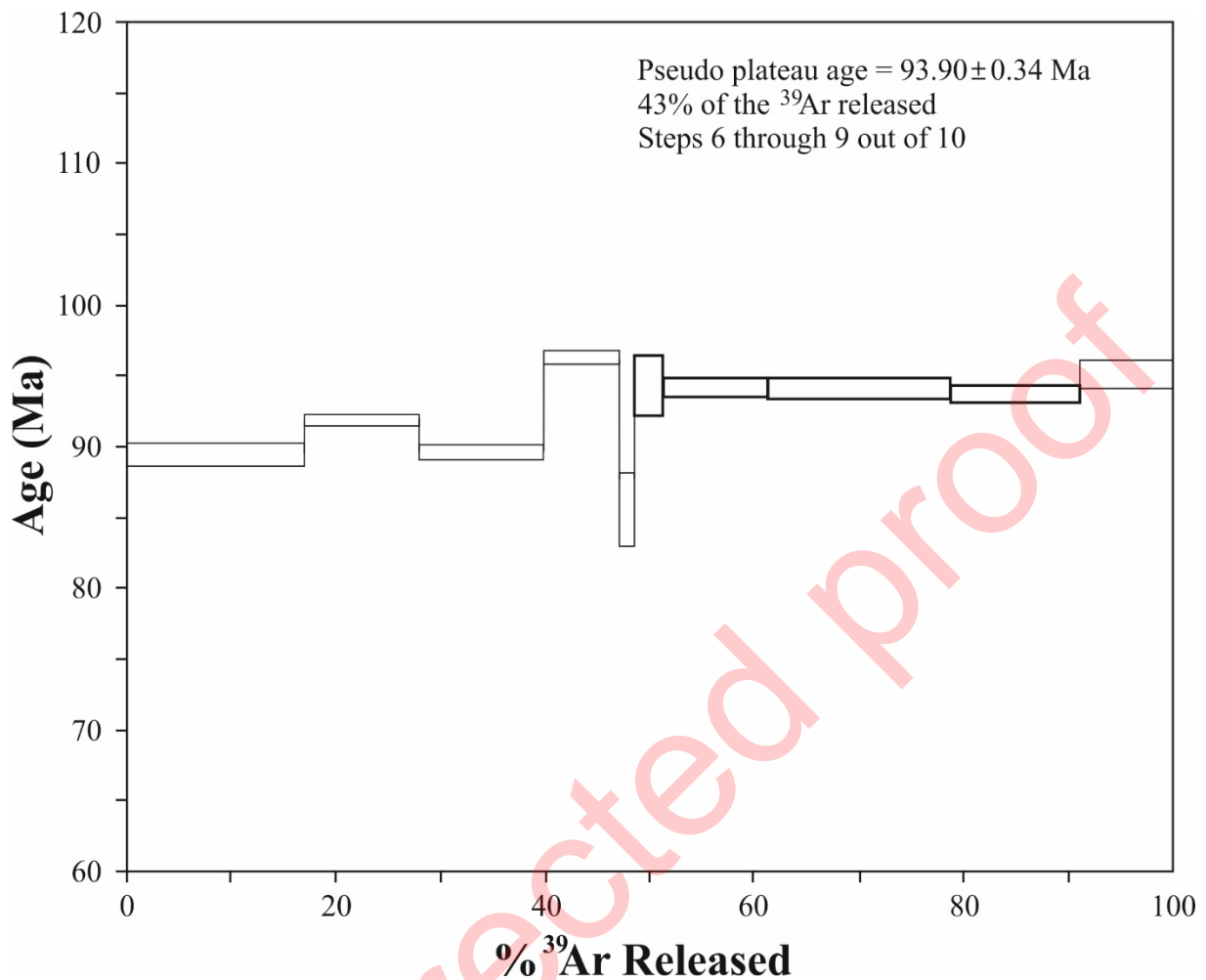
222



223

224 Figure 7- a, b) General view of the amphibolites of the Yenicekale metamorphics, c) tectonic relationships
 225 between the Yenicekale metamorphics (Kym) and the Marmaris ophiolite (Kmo) W of Mestan Hill, d)
 226 general view of the quartzite, quartz schist and calcschist, SE of Yenicekale village, e) an isolated
 227 diabase dyke intruding the amphibolites of the Yenicekale metamorphics (Kym), SE of Yenicekale
 228 village, f) thin section view of an amphibolite sample with a nematoblastic texture, under cross
 229 polarized light (Amp: amphibole, Plg: plagioclase).

230



232

233 Figure 8- Age spectrum for the amphibolite of the Yenicekale metamorphics.

234

235 Based on the analysis of the amphibolites, P-T conditions of $630\text{-}770^\circ\text{C}$ and 6 ± 1.5 kbar, corresponding to a
 236 burial depth of 18-20 km, are calculated for the metamorphism of these sub-ophiolitic metamorphic sole rocks
 237 (Elitok and Drüppel, 2008). The amphibolites show two different geochemical characters, alkaline and tholeiitic.
 238 According to this, the protoliths for alkaline amphibolites are within-plate type alkalin basalts, while the
 239 tholeiitic amphibolites are ocean island basalts (Elitok and Drippel, 2008; Parlak et al., 2019).

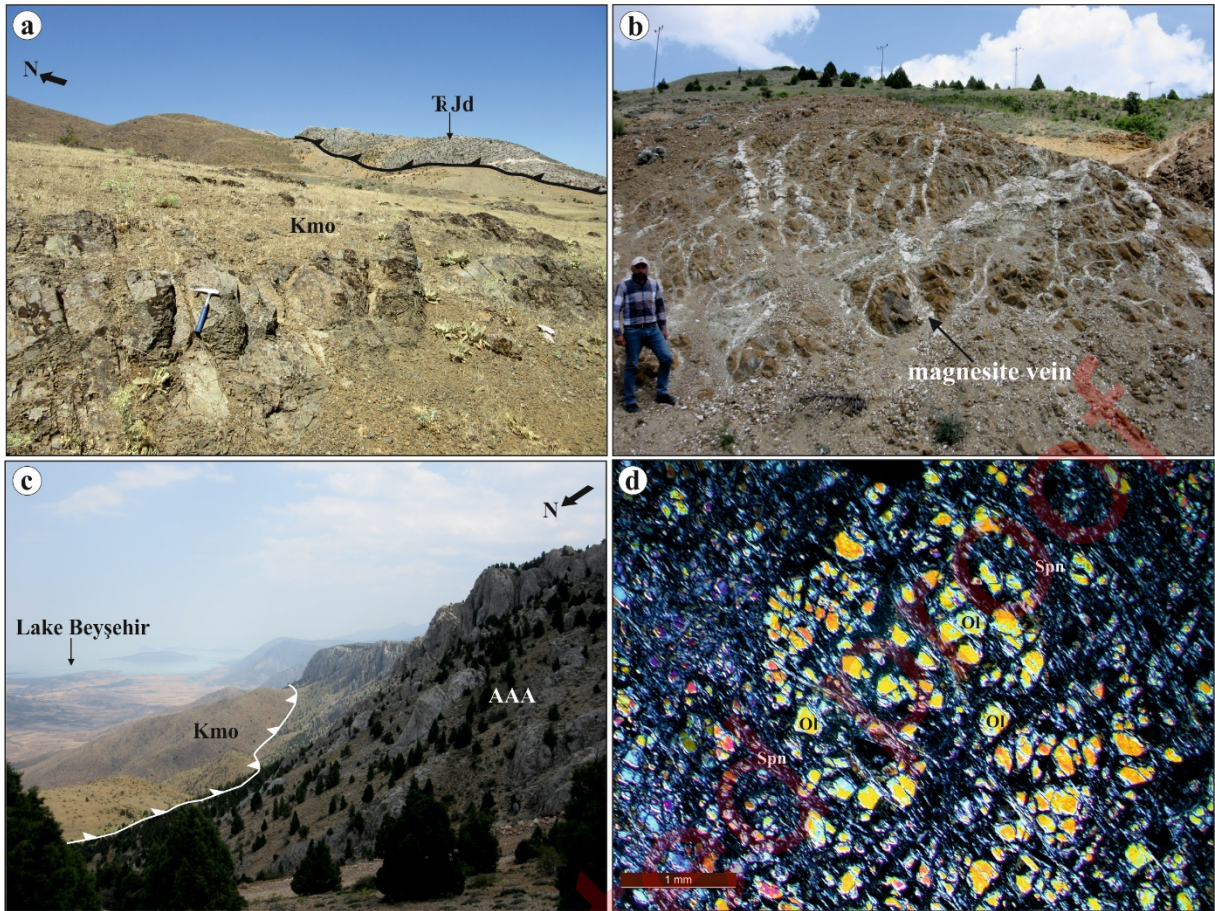
240 *Marmaris Ophiolite (Kmo)*: The ophiolitic rocks outcropping in the Lycian Nappes and the BHN, which are
 241 continuations of each other in southwestern Anatolia, have been defined under different names by various
 242 researchers. Various names have been given to the rock association, which consists mainly of dunite, harzburgite
 243 and serpentinized peridotite were referred to various names such as Beyşehir ophiolite (Ricou et al., 1975; Çelik

244 and Delaloye, 2006) and Hoyran ophiolite (Demirkol and Yetiş (1983-1984) within the BHN; ophiolites
245 (Andrew and Robertson, 2002) and peridotites (Elitok and Drüppel, 2008) within the Hoyran Nappes; peridotite
246 nappe (Graciansky, 1972), Yeşilova-Tefenni ophiolites (Sarıkaya and Seyrek, 1976), Yeşilova ophiolites (Sarp,
247 1976), Marmaris peridotite (Çapan, 1981) and Marmaris ophiolite (Ergen et al., 2021) within the Lycian Nappes.

248 The Marmaris ophiolite, whose lower and upper contacts are tectonic, is up to 1000 m thick. (Şenel, 1997). In
249 the study area, it tectonically overlies the Sultandağı Unit to the south of Şarkikaraağaç and the Anamas-Akseki
250 Autochthon, the Kızılcadağ mélangé and the Yenicekale metamorphics to the south of Yenicekale (Figure 9c).
251 On the other hand, the units belonging to the Gülbahar and Domuzdağ nappes rest on the ophiolites with a
252 tectonic contact.

253 The Marmaris ophiolite consists of serpentized dunite and harzburgite and isolated diabase dykes (Figure
254 9a). The most common rocks observed in this ophiolitic units are harzburgites, which are medium to coarse
255 grained, with green olivine and grey to black pyroxene minerals, brown on altered surfaces and blackish green to
256 green on fresh surfaces. Dunites, apart from olivine, also include orthopyroxene and chromite minerals, with a
257 mesh texture, light green to greenish grey in color, are less common than harzburgites. Serpentinization is
258 common, especially along fractures. Dunites and harzburgites are intruded by 0.5-2 m thick isolated diabase
259 dykes composed of plagioclase, clinopyroxene and opaque minerals with an ophitic texture. Zircon and titanite
260 minerals from these dykes, which characterize geochemically subduction-related island arc tholeiites, yielded U-
261 Pb ages of 87.5-102 Ma, while hornblende minerals yielded a ^{40}Ar - ^{39}Ar age of 91-93 Ma (Çelik et al., 2006).
262 Stockwork magnesite veins are widely observed in the ophiolites outcropping around Madenli village (Figure
263 9b).

264



265
 266 Figure 9- a) Tectonic relationship between the Marmaris ophiolite (Kmo) and the Dutdere Formation (T_{RJd}) of
 267 the Domuzdağ Nappe, NW of Sivri Hill, Yenicekale, b) stockwork magnesite veins in the ophiolites,
 268 NW of Eğirler, c) tectonic contact between the Marmaris ophiolite (Kmo) and the Anamas-Akseki
 269 Autochthon (AAA), NW of Lake Beyşehir, d) thin section view of a serpentinized dunite sample
 270 under cross polarized light (Ol: Olivine, Spn: Serpentine).
 271

272 The unit, which characterizes supra-subduction ophiolites, is accepted as Late Cretaceous in age based on
 273 radiometric data and geochemical analysis obtained from its isolated diabase dykes and metamorphic sole
 274 (Andrew and Robertson, 2002; Çelik et al., 2006; Elitok and Drüppel, 2008; Parlak et al., 2019; Ergen et al.,
 275 2021, Ergen, 2023).

276 2.4.2. Gülbahar Nappe

277 The Mesozoic allochthonous sequence of deep marine limestone, chert, radiolarite and mudstone and spilitic
 278 basalt is called the Gülbahar Nappe (Graciansky, 1972; Şenel et al., 1994). The Gülbahar Nappe and the Orluca

279 Formation from this nappe have been identified and mapped in this study for the first time in the south of Sultan
280 Dağları.

281 The Gülbahar Nappe is generally observed as blocks and slices of different sizes in the Kızılıcadağ mélangé.
282 Outcropping west of Ördekçi village and south of Salur (Şarkikaraağaç), the Gülbahar Nappe is represented in
283 the study area by the Orluca Formation. The aforementioned locations where the Orluca Formation is exposed
284 have been misinterpreted by previous researchers (e.g. Elitok and Drüppel, 2008; Parlak et al., 2019) as Upper
285 Cretaceous slope and basin deposits.

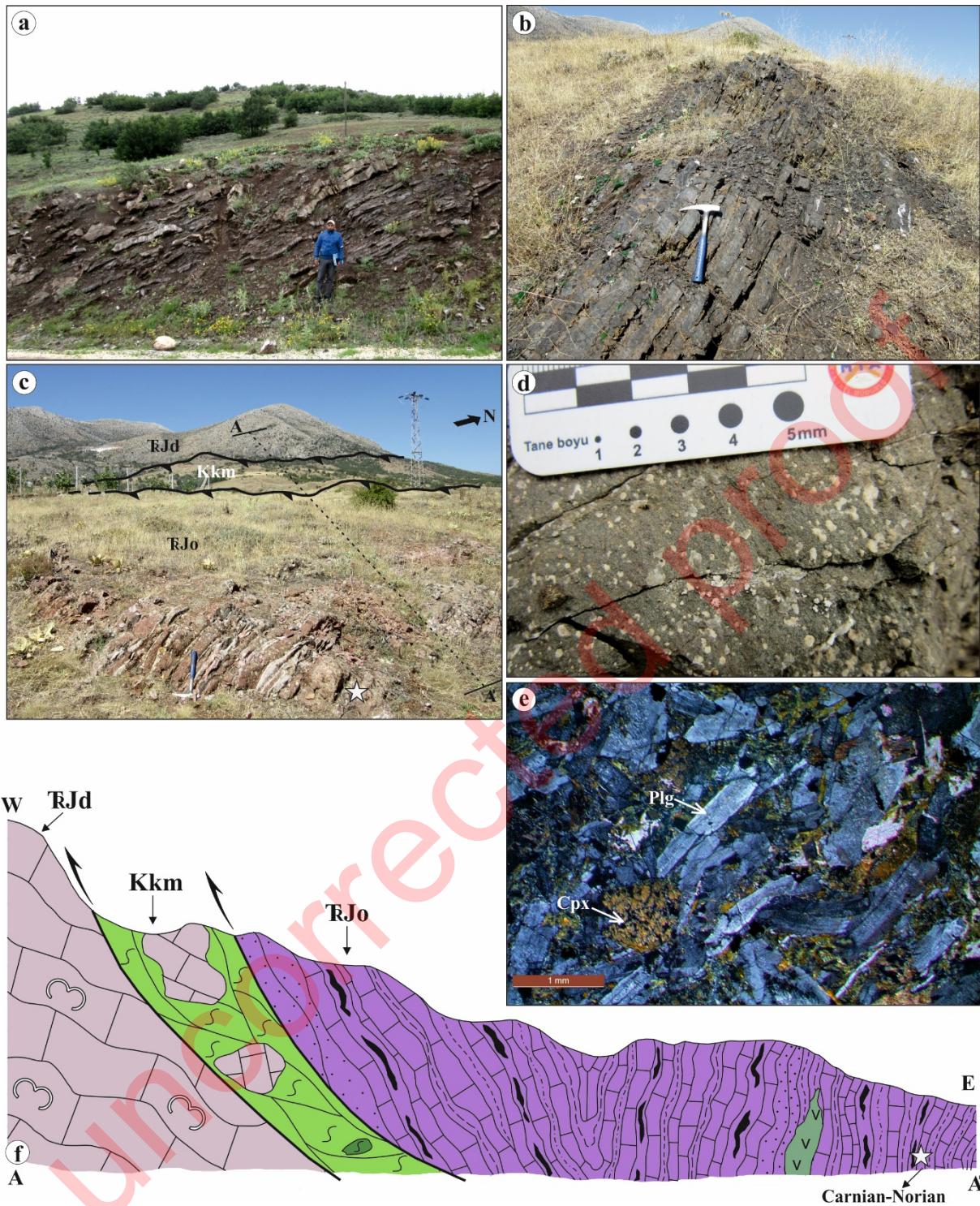
286 *Orluca Formation (T_RJo)*: The formation, which consists of volcanics, radiolarites, cherty micritic limestones,
287 mudstones and sandstones (Şenel, 1989), is exposed west of Ördekçi and south of Salur (Şarkikaraağaç).

288 The formation is composed of thin to medium-bedded, red, grey, green, intensely folded, deformed micritic
289 limestones with chert bands and nodules, and red, dark grey thin-bedded radiolarites, and green-greyish green,
290 medium- to thick-bedded sandstones and mudstones (Figures 10a-c). They are occasionally accompanied by
291 green, brown, fine- to medium-grained spilitic basalts (Figure 10d), which consist of plagioclase, clinopyroxene,
292 kaersutite, biotite, calcite and opaque minerals with an intersertal texture (Figure 10e). Sericitization and
293 argillization are common in plagioclase minerals, while chloritization is common in pyroxene minerals.
294 Radiolarites consist entirely of fossil radiolarian tests filled with very fine-grained siliceous minerals. The fact
295 that the formation consists of sandstone, mudstone, radiolarite, cherty micritic limestone with basic volcanic
296 intercalations indicates deposition in a slope and basin environment where both volcanism and turbidity currents
297 are occasionally active.

298 Tectonically overlying the Kızılıcadağ mélangé (Figures 10 c and 10f), the Orluca Formation is also observed
299 as blocks of various sizes in the mélangé.

300 In this study, radiolarian assemblages that contains *Capnuchosphaera* sp., *Tetraporobrachia* sp., *Sarla* sp.,
301 *Paronaella* sp. in the west of Ördekçi (coordinates: 36346310N/4213840E) and *Canoptum anulatum* Pessagno &
302 Poisson, *Lantus obesus* (Yeh), *Praeconocaryomma sarahae* Carter, *Bagotum* sp., *Katroma* sp., *Orbiculiforma*
303 sp., *Parahsuum* sp., *Pleesus* sp. in the south of Salur (coordinates: 349530N/4208601E) have been identified,
304 yielding the ages of Late Triassic and Pliensbachian-Toarcian (Early Jurassic), respectively.

305



306
307
308
309
310
311

Figure 10- a) Alternation of micritic limestone and mudstone in the Orluca Formation, S of Salur, b) dark grey radiolites, W of Ördekçi, c) tectonic relationships of the Orluca Formation with the Kızılcadağ mélange and the Dutdere Formation, NW of Ördekçi, d) a close-up view of the splitic basalts, e) thin section view of a basalt sample under cross polarized light (Cpx: Clinopyroxene, Plg: Plagioclase), f) a geological cross-section showing relations between the Dutdere Formation (TrJd), Kızılcadağ

312 mélange (Kkm) and Orluca Formation (T_{RJo}) (Note that the star indicates the stratigraphic position of
313 the dated paleontological sample).

314

315 2.4.3. Domuzdağ Nappe

316 The unit, which is observed as blocks and slices at various sizes within the Marmaris Ophiolite Nappe and
317 characterized by *Megalodon*-bearing neritic limestones, is recognized as the Domuzdağ Nappe (Poisson, 1977;
318 Ersoy, 1989; Şenel et al., 1994). The Middle Triassic-Early Jurassic Dutdere Formation represents the
319 Domuzdağ Nappe in the study area.

320 *Dutdere Formation (T_{RId})*: The Dutdere Formation (*sensu* Ersoy, 1989) consists mainly of grey, light grey,
321 beyaz and beige-colored, medium- to thick-bedded, *Megalodon* and algae-bearing and occasionally
322 recrystallized limestones, which are very fine-grained biomicrite, microsparite and sparry micrite. The
323 limestones, composed of calcite minerals and poorly preserved fossils in a micritic carbonate cement, are
324 sometimes recrystallized due to the intense tectonics caused by nappe movements. It contains cracks and
325 fractures developed in different directions and is observed as cataclastic and brecciated, especially at the nappe
326 contacts. Şenel et al. (1994) reported that pink to red, thin- to medium-bedded, ammonite-bearing cherty
327 limestones occur outside the study area above the *Megalodon*-bearing lower levels of the formation.

328 In the study area, the formation tectonically overlies the Marmaris ophiolite, Kızılcadağ mélange, and Orluca
329 Formation. The Kızılcadağ mélange is also observed over the Dutdere formation, depending on the tectonic
330 movements after its primary emplacement. One such contact relationship can be seen at the SE of Yenice kale.

331 Within the formation, which is easily recognized in the field by bearing *Megalodon* fossils, foraminifera such
332 as *Aulotortus* gr. *sinousus* (Weynschenk), *Aulotortus* sp., *Endoteba* sp., *Reophax* sp. have been determined in
333 this study at the south of Sultan Dağları, indicating a Late Triassic (Norian-Rhaetian) age. Şenel et al. (1989,
334 1994) assigned a Middle Triassic-Early Jurassic age to the formation, which is also accepted in this study, based
335 on the foraminiferal fauna obtained from the same formation at different locations in the Western
336 Taurides. Based on the lithological characteristics and fossil content, it can be inferred that the formation was
337 deposited in a shallow carbonate shelf environment.

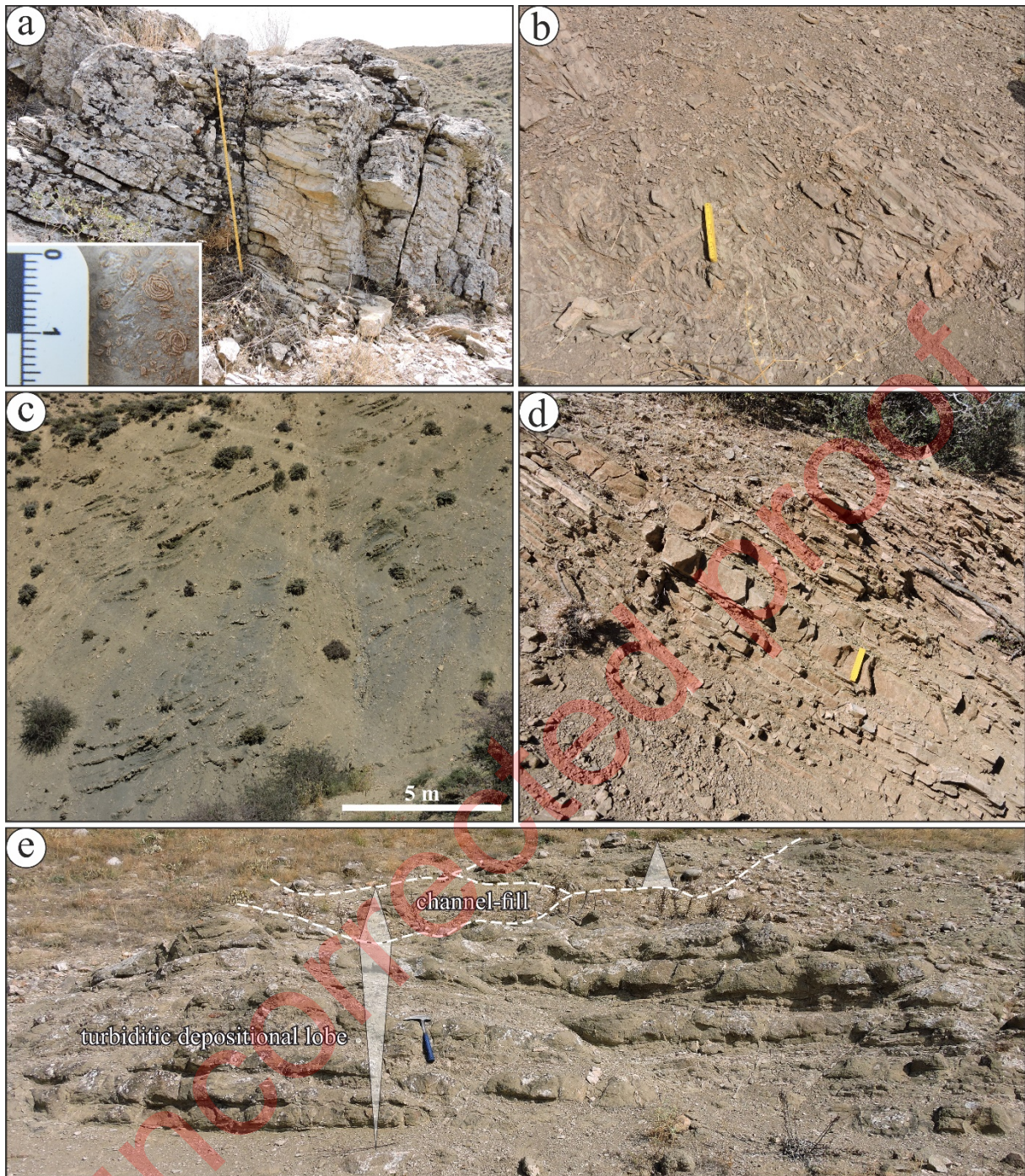
338 2.5. Cover rocks

339 2.5.1. Celeptaş Formation ($Pgpec$)

340 The Celeptaş Formation (sensu Demirkol, 1977) is mainly composed of thin-bedded limestones,
341 calcarenites, siltstones, mudstones, sandstones and subordinate conglomerates that form different facies and
342 facies associations (Figure 11). The thin-bedded, cream-coloured pelagic limestones and claret-coloured
343 calcarenite and biomicrite with abundant planktonic foraminifera are exposed in the north of the basin (Figures
344 11a, b). The fine-grained calcarenites are well-sorted and show planar parallel stratification and wave-ripple
345 cross-lamination (Figure 11b). They pass southwards into the interbedded mudstones, siltstones and sandstones,
346 forming mudstone- and sandstone-dominated sequences (Figures 11c, d, e).

347 Greenish-grey mudstones are laterally extensive and generally massive in the mudstone-dominated
348 sequences (Figure 11c). Very thin-bedded siltstones and very fine to fine sandstones interbedded with mudstones
349 are generally 0.5-5 cm thick, and in lesser amounts up to 15 cm. Sedimentary structures include planar parallel
350 stratification, normal grading and current ripple cross-lamination.

351



352
 353 Figure 11- Facies details of Dursunlu Formation, a) Thin-bedded pelagic limestones with *Nummulites* fossils and
 354 b) claret-coloured calcarenite and biomicrite, c) Massive mudstones of the basin-plain hemipelagic
 355 deposits interbedded with siltstone and sandstone turbidites, d) The sandstone-dominated sequence
 356 consists mainly of Bouma-type Tbc and lesser amounts of Tabc turbidites, e) The coarsening- and
 357 thickening-upward bed packages of the turbiditic depositional lobes are erosionally overlain by the
 358 fining-upwards bedsets of the channel-fill deposits. The ruler is 1 m in figure a and 10 cm in figures b
 359 and d, the hammer is 33 cm.

360

361 The sandstone-dominated sequence consists mainly of grey to light brown sandstones and siltstones
362 interbedded with grey mudstones (Figure 11d). The tabular sandstones, which are generally 10-30 cm thick,
363 contain mainly Bouma-type Tbc and lesser amounts of Tabc turbidites. Other sedimentary structures include
364 flute and groove marks, load casts, convolute laminations and some trace fossils. The interbedded sandstones,
365 siltstones and mudstones, form coarsening- and thickening-upward bed packages a few metres thick (Figure
366 11e). These are erosionally overlain by lenticular channel-fill deposits in the axial part (Figure 11e). The fining
367 upward bedset of the channel-fill deposits consist of coarse sandstones to granule conglomerates, rich in pebble
368 gravels at the base.

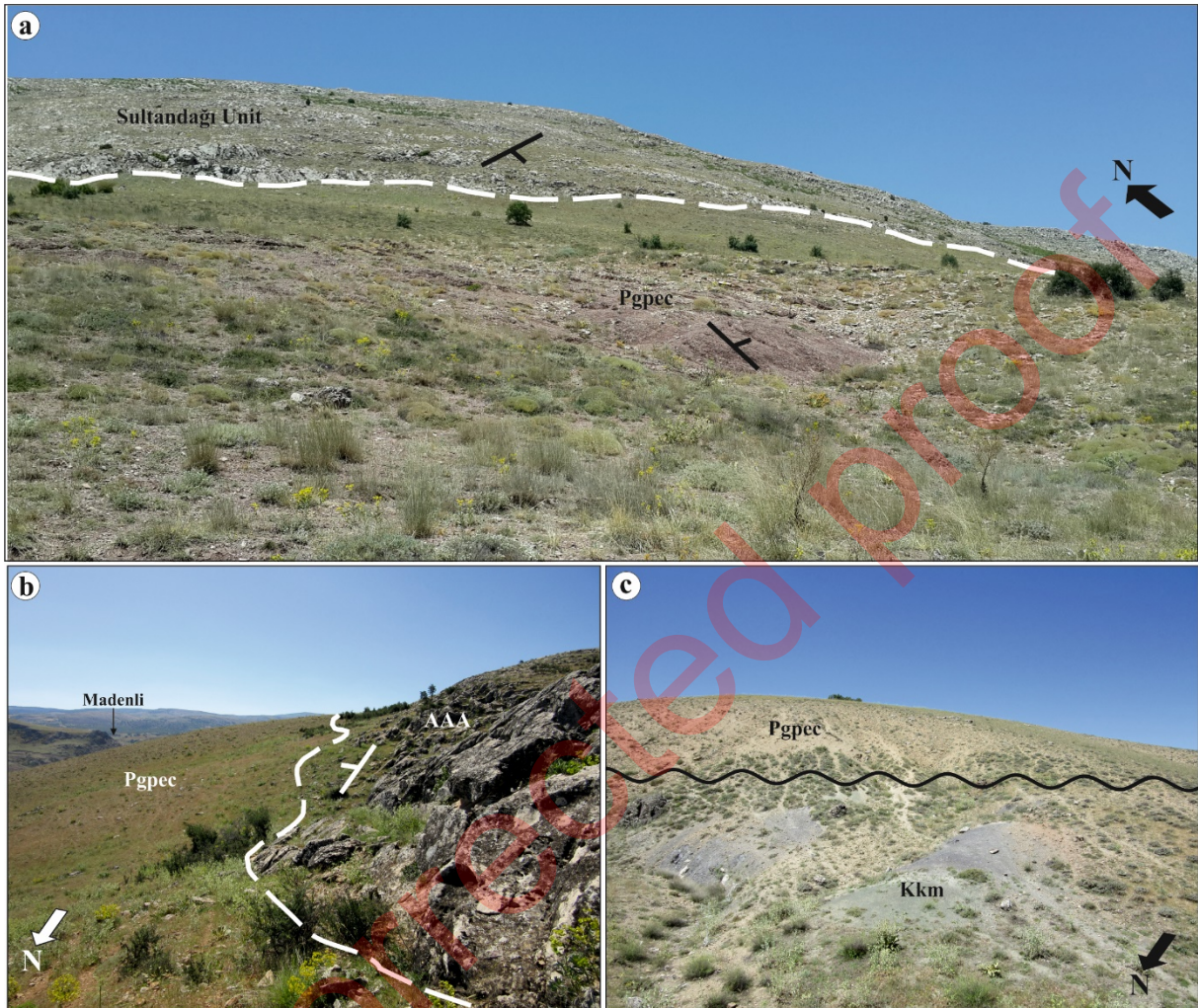
369 The *Nummulites*-bearing pelagic limestones and biomicrites, rich in planktonic foraminifers, indicate a
370 neritic carbonate platform formed on the basin-margin narrow shelf. The calcarenites are interpreted to represent
371 wave-worked, lower shoreface to offshore transition deposits (cf. Clifton, 1981; Dott and Bourgeois, 1982). The
372 mudstones are interpreted to be basin-plain hemipelagic deposits interlayered with thin siltstone and sandstone
373 turbidites in the mudstone-dominated bed packages. The graded sandstone beds with planar stratification are
374 tractional deposits of low-density turbidity currents (Bouma, 1962; Lowe, 1982; Kneller, 1995). The sandstone-
375 dominated coarsening-upwards bed packages are interpreted as turbiditic depositional lobes and the overlying
376 fining-upwards bedsets as channel-fill deposits. The sedimentary facies of these deposits indicate high- and low-
377 density turbidity currents. The composition of the sandstone and the pebbles indicates that the sand grains and
378 clasts are of ophiolitic origin.

379 The Celeptaş Formation unconformably covers the Sultandağı Unit, the Anamas-Akseki Autochthon
380 and the BHN (Figure 12), while it is tectonically overlain in places by the BHN (Figure 13).

381 The results of the planktonic foraminiferal analyses performed on the marine mudstone samples from
382 Hodulca Hill northwest of Yalvaç (327382E/4244438N), north of Celeptaş village (327382E/4244438N) and
383 south of Yenicekale (341350E/4214700N) (Figures 2, 3) are given below.

384 Among the abundant planktonic foraminiferal assemblages of the Celeptaş Formation, the species such
385 as *Globanomalina pseudomenardii* and *Acarinina soldadoensis* in the Thanetian, *Morozovella subbotinae* and
386 *Morozovella velascoensis* in the late Thanetian, *Morozovella edgari* and *Morozovella gracilis* in the early
387 Ypresian, *Morozovella lensiformis* and *Morozovella aragonensis* in the Ypresian, *Acarinina bullbrooki*,
388 *Acarinina cuneicamerata* and *Turborotalia frontosa* in the late Ypresian to Lutetian levels have been identified

389 in a stratigraphical order as markers. The age of the Celeptaş Formation has been assigned as Late Paleocene-
390 Lutetian based on this planktonic foraminiferal content.
391



392
393 Figure 12- a) The unconformable contact between the Celeptaş Formation and the Middle Jurassic-Upper
394 Cretaceous recrystallized limestones of the Sultandağı Unit, near Hodulca Hill, Yalvaç, b)
395 unconformable contacts between the Celeptaş Formation and Jurassic-Cenomanian limestones of the
396 Anamas-Akseki Autochthon (AAA) and c) Kızılcaadağ mélangé (Kkm) of the BHN, north of Madenli.
397



398

399 Figure 13- a) Thrust contact between the Kızılcadağ mélangé of the BHN and the Celeptaş Formation, SE of
 400 Yenice kale, b) close-up of the first figure showing folds.

401

402 *2.5.2. Yalvaç Basin*

403 The Yalvaç Basin, which is formed of terrestrial and lacustrine deposits, is a triangular molasse basin that
 404 extends in a NW-SE direction between the Sultan Dağları and the Anamas Mountains (Yağmurlu, 1991; Ilgar et
 405 al., 2021). Deposits of the basin are alluvial fan, lacustrine clastic and carbonate sediments. The formation of the
 406 Yalvaç Basin, which began to open after nappe emplacement as a result of orogenic collapse, is known to have
 407 been influenced by the break-up or roll-back of the Southern Neotethys slab during the Early Miocene (Koçyiğit
 408 and Devceci, 2007; Koçyiğit et al., 2013; Koç et al., 2016; Ilgar et al., 2021). The sediments of the Yalvaç Basin
 409 unconformably overlie all pre-Miocene units in the region.

410 **3. Discussions**

411 The formation and emplacement processes of the BHN are important in revealing the geodynamic evolution
 412 of the region. The generally accepted aspect is that the BHN was formed as a result of horizontal movements due
 413 to the closure of the northern branch of the Neotethys Ocean (İzmir-Ankara-Erzincan and/or Inner Tauride
 414 Ocean) and settled in the region by thrusting over the Sultan Dağları from north to south during the Late
 415 Cretaceous-Eocene (Özgül, 1984; Andrew and Robertson, 2002; Çelik and Delaloye, 2006; Elitok and Drüppel,
 416 2008).

417 There are several critical issues in dating nappes formed by oceanic subduction processes such as the BHN,
 418 the most important of which are the age of the sub-ophiolitic metamorphic rocks, the age of the matrix and

419 blocks of the mélangé and the age of the cover of the nappes. The formation of nappes begins with the
420 development of the sub-ophiolitic metamorphic rocks, which represent the onset of subduction, while it ends
421 with the youngest age obtained from the matrix in the mélangé. The emplacement time, on the other hand, is
422 constrained by the youngest unit the nappes thrust over and the overlying oldest unit.

423 The sub-ophiolitic metamorphic rocks, which formed during the onset of subduction, are widely accepted as
424 definitive indicators of subduction initiation ages, with metamorphic ages derived from their amphibolites (Çelik
425 and Delaloye, 2006). In this context, the 93.90 ± 0.34 Ma (Cenomanian-Turonian boundary) age data obtained
426 from the Yenicekale metamorphics is accepted as the onset of the formation of the BHN (Figure 14a).

427 The ages obtained from the blocks and matrix of the mélangé are another significant parameter related to the
428 formation of the mélangé. Accordingly, the occurrence of Upper Triassic Domuzdağ Nappe, Upper Triassic-
429 Lower Jurassic Gülbahar Nappe and Upper Cretaceous Marmaris Ophiolite Nappe blocks and slices within the
430 Kızılcadağ mélangé and the determination of late Maastrichtian planktonic foraminifera from the matrix of the
431 mélangé indicate that the formation of the BHN lasts possibly from the Turonian to the late Maastrichtian.

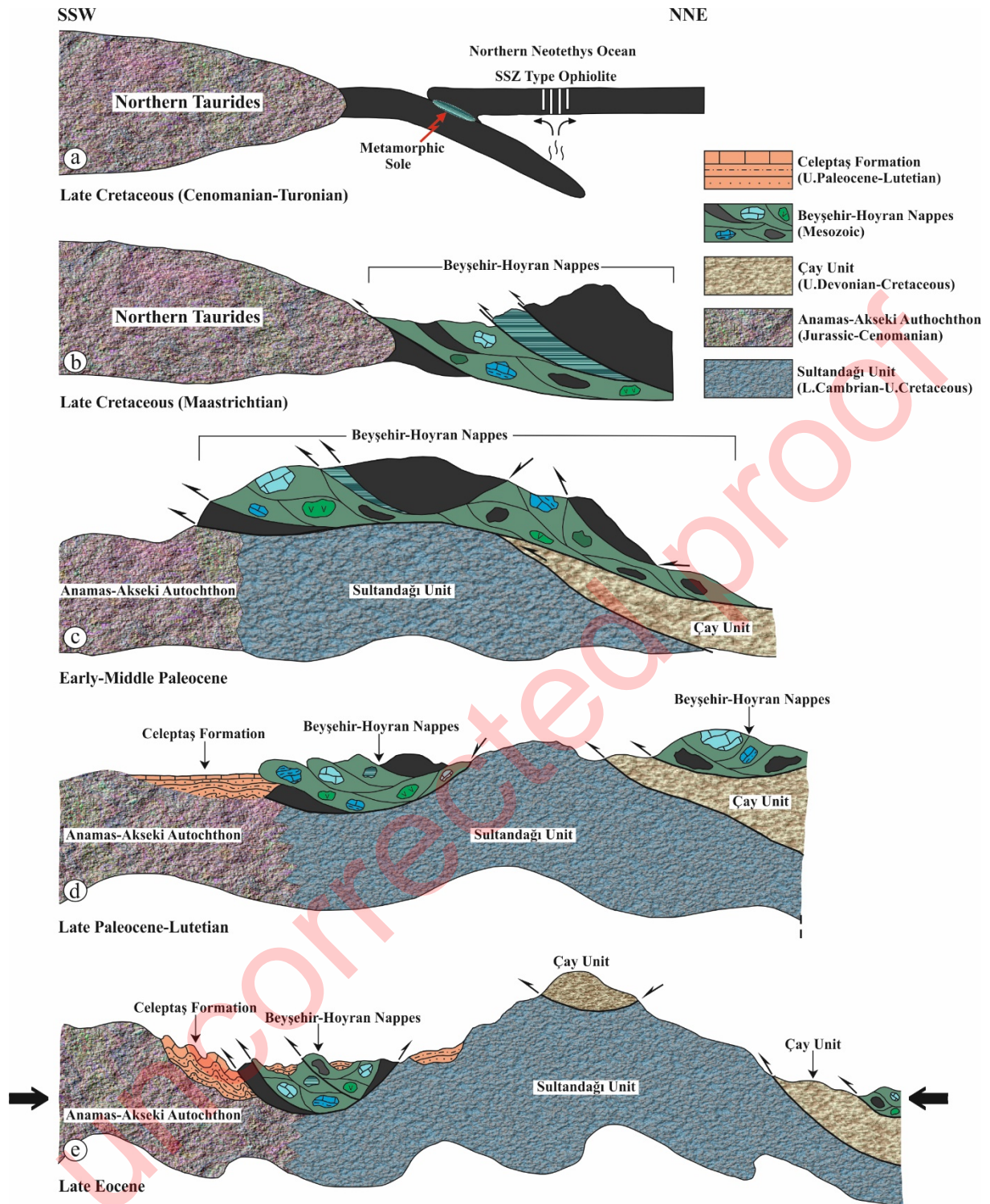
432 The basin type in which the Celeptaş Formation was deposited has been inferred from the sedimentary
433 characteristics of the formation and its tectonostratigraphic relationship with the surrounding units. The rapid
434 transition of the neritic carbonate and offshore transition deposits of the Celeptaş Formation into the deep marine
435 facies indicates a narrow shelf and increased supply of terrigenous sediments to the basin. In addition, intense
436 compressional tectonic deformation during and after deposition suggests that the sediments were deposited in a
437 tectonically controlled basin. Therefore, taken together, we have interpreted the Celeptaş Formation as being
438 deposited in a foreland basin that was fed by and developed in front of the BHN. The flexural subsidence of the
439 basin floor, driven by the crustal load of the BHN, led to the development of sediment accommodation space.
440 Tectonic loading from the north resulted in the development of a deep-marine environment. Thus, the turbidite
441 deposits of the Celeptaş Formation both transgressively overlie the BHN and, in the ongoing process, the BHN
442 tectonically overlies the Celeptaş Formation from north to south (Figure 14d).

443 The first emplacement age of the BHN must be younger than the tectonically underlying early Cambrian-
444 Late Cretaceous Sultandağı Unit and the Jurassic-Cenomanian Anamas-Akseki Autochthon, while it must be
445 older than the late Paleocene-Lutetian Celeptaş Formation, the common cover of the parautochthonous and
446 allochthonous units in the region, thus pointing to an early-middle Paleocene emplacement age (Figure 14c). The

447 ongoing movements of the BHN and its settlement in the basin caused the synsedimentary deformation of the
448 Celeptaş Formation.

449 Şenel (1991) argued for the presence of a Paleocene-Lutetian common marine basin extending from the
450 Lycian Nappes towards Seydişehir along the Isparta Angle. These data also support the idea that the BHN was
451 not emplaced in the region during late Eocene, contrarily, but already existed there before the late Paleocene.
452

Uncorrected proof



453

454 Figure 14- Geological sections illustrating the evolution of the BHN during the Late Cretaceous to late Eocene
 455 period.

456

457 The stratigraphic studies and geological mapping carried out in the region during this study, as well as the
 458 age data obtained from both the BHN and the Celeptaş Formation, helped to reinterpret the Late Cretaceous-

459 Eocene geological evolution of the region. The initiation of the northward subduction of the northern branch of
460 the Neotethys Ocean led to the formation of SSZ-type ophiolites (Marmaris ophiolite) and consequently to the
461 development of sub-ophiolitic metamorphic sole (Yenicekale metamorphics) at the Cenomanian-Turonian
462 boundary (Figure 14a). During the Late Cretaceous-early Paleocene, from north to south, the BHN thrust over
463 the Çay Unit and the Çay Unit thrust over the Sultandağı Unit (Figures 14b-c). In the early Paleocene, the
464 BHN crossed the Sultan Dağları and reached the Anamas-Akseki Autochthon (Figure 14c). During this period,
465 the rocks of the Sultandağı and Çay units underwent both deformation and low-grade metamorphism depending
466 on the emplacement of the BHN (Figure 14c). Following this process, the Celeptaş Formation was deposited in
467 the foreland basin, which developed in the south of Sultan Dağları, in the late Paleocene-Lutetian period.
468 Following this process, the Celeptaş Formation was deposited in the foreland basin that developed in the south of
469 Sultan Dağları in the late Paleocene-Lutetian period (Figure 14d).

470 The Celeptaş Formation was folded due to the tectonic movements, probably occurred in the late Eocene, and
471 subsequently was overthrust in places by units of the BHN. These can be considered as secondary thrusts after
472 the primary emplacement (Figure 14e).

473 **4. Conclusions**

474 The BHN, which extends as a NW-SE belt to the south of Sultan Dağları, consists of allocthonous masses
475 such as the Marmaris Ophiolite Nappe, Gülbahar Nappe and Domuzdağ Nappe. The Marmaris ophiolite nappe
476 (Upper Cretaceous) is formed by three subunits as the Marmaris ophiolite, the Kızılcadağ mélangé and the
477 Yenicekale metamorphics. The Marmaris ophiolite is composed of dunite, harzburgite, serpentinite and isolated
478 diabase dykes, while the Kızılcadağ mélangé is composed by blocks of different ages and lithologies contained
479 in an ophiolitic/sedimentary matrix. The Yenicekale metamorphics are characterized by sub-ophiolitic
480 metamorphic sole rocks such as amphibolites, quartzites and calcschists.

481 The Gülbahar Nappe is represented by the Late Triassic-Early Jurassic Orluca Formation, which is composed
482 of deep marine mudstones, cherts, radiolarites, micritic limestone and basic volcanics. The Orluca Formation,
483 which has been identified for the first time at the south of Sultan Dağları, yielded paleontological ages of
484 Carnian-Norian (Late Triassic) and Pliensbachian-Toarcian (Early Jurassic) from its micritic limestones and
485 radiolarites.

486 In addition, we obtained a $^{40}\text{Ar}-^{39}\text{Ar}$ age of 93.90 ± 0.34 Ma (Cenomanian-Turonian boundary) from the
487 hornblende minerals of amphibolites from the Yenicekale metamorphics. Tectonic processes, which were

488 triggered by and occurred immediately following the formation of the metamorphic sole during the
489 aforementioned time started the formation of the nappes. We therefore accepted that the Turonian time should be
490 the onset of the formation of the BHN.

491 On the other hand, the late Maastrichtian age, which is obtained from the mudstones in the matrix of the
492 Kızılcadağ mélangé, is considered to mark the end of the formation of the BHN.

493 The evaluation of the stratigraphic, palaeontological and radiometric data together reveals that the formation
494 of the BHN began in the Turonian and ended in the Late Maastrichtian. The Late Paleocene-Lutetian Celeptaş
495 Formation unconformably overlies the Sultandağı Unit, Anamas-Akseki Autochthon and BHN as common cover
496 in the study area. This clearly indicates that the BHN was emplaced in the region during the early-middle
497 Paleocene. The BHN reached its final position as a result of late Eocene movements.

498 **5. Acknowledgements**

499 This study was carried out in the scope of “Geology and Geodynamic Evolution of the Sultan Dağları”
500 project (Project code: 2016-30-14-05) by the Department of Geological Research of the General Directorate of
501 Mineral Research and Exploration (MTA). All necessary permissions for this publication have been obtained
502 from MTA.

503 The authors are grateful to Dr. Havva Soycan, Dr. Burcu Coşkun Tunaboşlu, Dr. Erkan Ekmekçi for the
504 palaeontological determinations and to Dr. Meral Gürel, Aylin Paçala and Banu Türkmen Bozkurt for the
505 petrographic examinations of the samples. The manuscript was critically reviewed by Prof. Alastair Robertson
506 and two anonymous reviewers, whose constructive comments are much appreciated.

507

508

509

510

511

512

513

514

515 **6. References**

- 516 Andrew, T., Robertson, A. H. F. 2002. The Beyşehir–Hoyran–Hadim Nappes: genesis and emplacement of Mesozoic
517 marginal and oceanic units of the northern Neotethys in southern Turkey. *Journal of the Geological Society*,
518 London, 159, 2002, 529–543.
- 519 Bouma, A.H. 1962. *Sedimentology of some Flysch Deposits: A Graphic Approach to Facies Interpretation*. Elsevier,
520 Amsterdam, 168.
- 521 Candan, O., Çetinkaplan, M., Oberhänsli, R., Rimmelé, G., Akal, C. 2005. Alpine high-P/low-T metamorphism of the Afyon
522 Zone and implications for the metamorphic evolution of Western Anatolia, Turkey. *Lithos*, Volume 84, Issues 1–2,
523 September 2005, 102-124.
- 524 Clifton, H.E. 1981. Progradational sequences in Miocene shoreline deposits, southeastern Caliente Range, California. *J.*
525 *Sediment. Petrol.*, 51, 165–184.
- 526 Çapan, U. Z. 1981. Toros Kuşağı'na ait beş ofiyolit masifinde (Marmaris, Mersin, Pozantı, Pınarbaşı, Divriği) Major Element
527 Analizlerinin İstatistiksel Yorumu, Ortalama Değerlerin Karşılaştırılması. *Yerbilimleri*, No: 7.
- 528 Çelik, Ö.F., Delaloye, M. 2006. Characteristics of ophiolite-related metamorphic rocks in the Beyşehir ophiolitic mélange
529 (Central Taurides, Turkey), deduced from whole rock and mineral chemistry. *Journal of Asian Earth Sciences*, 26,
530 461-476.
- 531 Çelik, Ö.F., Delaloye, M., Feraud, G. 2006. Precise ^{40}Ar - ^{39}Ar ages from the metamorphic sole rocks of the Tauride Belt
532 Ophiolites, southern Turkey: Implications for the rapid cooling history. *Geol. Mag.* 143 (2):213–227.
- 533 Dedeoğlu Yıldız, D., Yılmaz, K., Aysal, N. 2021. Petrology and zircon U-Pb geochronology of mafic - intermediate dykes in
534 the West-Central Taurides: Implications for magma source during the Late Precambrian – Early Palaeozoic.
535 *International Geology Review* 64 (1).
- 536 Demirkol, C. 1977. Yalvaç-Akşehir dolayının jeolojisi. Doçentlik Tezi, Selçuk Üniversitesi Fen Fak. Yerbilimleri Bölümü.
537 Konya.
- 538 Demirkol, C., Yetiş, C. 1983-1984. Hoyran Gölü kuzeyinin stratigrafisi. *MTA Dergisi*, 101-102, 1–13.
- 539 Dott, R.H. JR, Bourgeois, J. 1982. Hummocky stratification: significance of its variable bedding sequences. *Geol. Soc. Am.*
540 *Bull.*, 93, 663–680.
- 541 Elitok, Ö., Drüppel, K. 2008. Geochemistry and tectonic significance of metamorphic sole rocks beneath the Beyşehir-
542 Hoyran ophiolite (SW turkey). *Lithos*, 100, 322-353.

- 543 Ergen, A. 2023. Sultan Dağları'nın Doğanhisar (Konya)-Gelendost (Isparta) arasında kalan güney bölümünün tektono-
544 stratigrafisi ve yapısal özellikleri. Doktora Tezi, Konya Teknik Üniversitesi, Lisansüstü Eğitim Enstitüsü, Jeoloji
545 Mühendisliği Anabilim Dalı, 229 (unpublished).
- 546 Ergen, A., Bozkurt, A., Ilgar, A., Tuncay, E., Doğan, A. 2021. Sultan Dağları'nın Jeolojisi ve Jeodinamik Evrimi, MTA
547 Rapor No: 13958, 241, Ankara (unpublished).
- 548 Ergen, A., Ilgar, A., Bozkurt, A., Tuncay, E., Soyacan, H., Hakyemez, A. 2020. Sultandağları Güneyinde Beyşehir-Hoyran
549 Naplarının Tektono-Stratigrafisi", 73. Türkiye Jeoloji Kurultayı, 158-159, Ankara.
- 550 Ersoy, Ş. 1989. Fethiye (Muğla)-Göhlhisar (Burdur) arasında Güney Dağı ile Kelebekli Dağı ve dolayının jeolojisi, Doktora
551 Tezi, İ.Ü. Fen. Bil. Enst., 246.
- 552 Görür, N., Oktay, F. Y., Seymen, İ. and Şengör, A. M. C. 1984. "Palaeotectonic evolution of the Tuzgölü basin complex,
553 Central Turkey: Sedimentary record of a Neo-Tethyan closure". In The geological evolution of the eastern
554 Mediterranean, Geol. Soc. Lond. Spec. Publ. no. 17 Edited by: Dixon, J. E. and Robertson, A. H. F. 467-482.
- 555 Görür, N., Şengör, A. M. C., Akkök, R., Yılmaz, Y. 1983. Sedimentological data regarding the opening of the northern
556 branch of the Neo-Tethys in the Pontides. Türkiye Jeoloji Kurumu Bülteni, 26, 11-20 [in Turkish].
- 557 Graciansky, P. de. 1972 Recherches géologiques dans le Taurus Lycien occidental. (Theses) Univ. De Paris-Sud Centre
558 d'Orsay, 762.
- 559 Gutnic, M., Keller, D., Monod, O. 1968. Decouverte de nappes de charriage dans le nord du Taurus occidental (Turquie
560 mSridionale), C.R. Acad. Sci., Paris 226, 988-901.
- 561 Güngör, T. 2013. Kinematics of the Central Taurides during Neotethys closure and collision, the nappes in the Sultan
562 Mountains, Turkey, Int. Journal Earth Science, 102: 1381-1402.
- 563 Ilgar, A., Ergen, A., Tuncay, E., Bozkurt, A. 2021. Basin margin tectonics and morphology as controls of delta type and
564 architecture: Examples from the Mio-Pliocene Yalvaç Basin (SW Turkey), Turkish Journal of Earth Sciences, 30:
565 516-535.
- 566 Ketin, İ. 1966. Anadolu'nun tektonik birlikleri, MTA Dergisi, 66, 20-36, Ankara.
- 567 Kneller, B. 1995. Beyond the turbidite paradigm: physical models for deposition of turbidites and their implications for
568 reservoir prediction. Geological Society, London, Special Publications 94, 31-49.
- 569 Koç, A., Kaymakçı, N., van Hinsbergen, D. J. J., Vissers, R. L. M. 2016. A Miocene onset of the modern extensional regime
570 in the Isparta Angle: constraints from the Yalvaç double dagger Basin (southwest Turkey), International Journal of
571 Earth Sciences, 105, 1, 369-398.

- 572 Koçyiğit, A., Deveci, Ş. 2007. Çukurören- Çobanlar (Afyon) arasındaki deprem kaynaklarının (Aktif fayların) belirlenmesi,
573 TÜBİTAK, Proje No: 106Y209, 71, Ankara.
- 574 Koçyiğit, A., Gürboğa, Ş., Kalafat, D. 2013. Nature and onset of neotectonic regime in the northern core of Isparta angle, SW
575 Turkey. *Geodinamica Acta*, 25 (1-2), 52-85.
- 576 Linnemann, U., Pereira, F., Jeffries, E.T., Drost, K., Gerdes, A. 2008. The Cadomian Orogeny and the opening of the Rheic
577 Ocean: the diachrony of geotectonic processes constrained by LA-ICP-MS U-Pb zircon dating (Ossa-Morena
578 and Saxo-Thuringian Zones, Iberian and Bohemian Massifs). *Tectonophysics* 461, 21–43.
- 579 Lowe, D.R. 1982. Sediment gravity flows, II. Depositional models with special reference to the deposits of high-density
580 turbidity currents. *J. Sediment. Petrol.*, 52, 279–297.
- 581 Mackintosh, P.W., Robertson, A.H.F. 2009. Structural and sedimentary evidence from the northern margin of the Tauride
582 platform in south central Turkey used to test alternative models of Tethys during Early Mesozoic time.
583 *Tectonophysics* 473, 149–172.
- 584 Monod, O. 1977. Recherches Géologique Minéralogique et Géochimique des Bouxites de la Région d'Akseki Seydişehir
585 (Taurus Occidental-Turquie). These Üniv. Pire et Marie Curie, Paris.
- 586 Nance, R.D., Gutierrez-Alonso, G., Keppie, J.D., Linnemann, U., Murphy, J.B., Quesada, C., Strachan, R.A., Woodcock,
587 N.H. 2010. Evolution of the Rheic Ocean. *Gondwana Research* 17, 194-222.
- 588 Okay, A.I. 1984. Kuzeybatı Anadolu'da yer alan metamorfik kuşaklar, in Proceedings, Ketin Symposium, Ankara, February,
589 1984 (83-92).
- 590 Okay, A.I., Tüysüz, O. 1999. Tethyan sutures of northern Turkey. In *The Mediterranean Basins: Tertiary Extension Within*
591 *the Alpine Orogen* (eds B. Durand, L. Jolivet, F. Horváth & M. Séranne), pp. 475–515, Geological Society of
592 London, Special Publication no. 156.
- 593 Özgül, N. 1976. Torosların bazı temel jeolojik özellikleri, *Türkiye Jeoloji Kurumu Bülteni*, 19/1, 65-67.
- 594 Özgül, N. 1984. Stratigraphy and tectonic evolution of the Central Taurides. *International Symposium on the Geology of the*
595 *Taurus Belt*. (eds. Tekeli, O. and Göncüoğlu, M.C.) 77-90, Ankara.
- 596 Özgül, N. 1997. Stratigraphy of the tectonostratigraphical units around Hadım–Bozkır–Taşkent region, northern part of the
597 Central Taurides. *Bulletin of Mineral Resources Exploration (Turkey)*, 119, 113–174.
- 598 Özgül, N., Bölükbaşı, S., Alkan, H., Öztaş, Y., Korucu, M. 1991. Sultandağları-Sandıklı-Homa-Akdağ yöresinin jeolojisi.
599 *Türkiye Petrolleri Anonim Ortaklığı Rapor No: 3028*, Ankara.

- 600 Parlak, O., Dunkl, I., Karaođlan, F., Kusky, T. M., Zhang, C., Wang, L., Koepke, J., Billor, Z., Hames, W.E., ŐimŐek, E.,
601 ŐimŐek, G., ŐimŐek, T., Őztürk, S.E. 2019. Rapid cooling history of a Neotethyan ophiolite: Evidence for
602 contemporaneous subduction initiation and metamorphic sole formation. Geological Society of America Bulletin,
603 vol.131, 2011-2038.
- 604 Parlak, O., Rızaođlu, Bađcı, U., Karaođlan, F., Hock, V. 2009. Tectonic significance of the geochemistry and petrology of
605 ophiolites in southeast Anatolia, Turkey. Tectonophysics 473, 173-187.
- 606 Poisson, A. 1977. Recherches geologiques dans les Taurus occidentales, Turquie. PhD Thesis, Universite de Paris-Sud,
607 Orsay.
- 608 Poisson, A., Akay, E., Dumont, J.F. & Uysal, S. 1984. The Isparta Angle: a Mesozoic paleorift in the Western Taurides. In:
609 Geology of the Taurus Belt (Ed. by O. Tekeli & M.C.Goncüođlu), 11–26, MIT, Ankara.
- 610 Pourteau, A., Candan, O., Oberhansli, R. 2010. High-Pressure metasediments in central Turkey: constraints on the
611 Neotethyan closure history. Tectonics, 29.
- 612 Pourteau, A., Sudo, M., Candan, O., Lanari, P., Vidal, O., Oberhansli, R. 2013. Neotethys closure history of Anatolia: insight
613 from ⁴⁰Ar–³⁹Ar geochronology and P–T estimation in high-pressure metasediments, J Metamorph Geol., 31, 585–
614 606.
- 615 Ricou, L.E., Argyriadis, I. et Marcoux, J.. 1975. L'axe calcaire du Taurus, un alignement de fenetres arabo - africaines sous les
616 nappes a materiel radiolaritique, ophiolitique et metamorphic. Bull. soc. Geol. France, 17 : 1024 -1044.
- 617 Robertson, A. H. F., Dixon, J. E. 1984. Introduction; Aspects of the Geological Evolution of the Eastern Mediterranean. In
618 The Geological Evolution of the Eastern Mediterranean (eds J. E. Dixon & A. H. F. Robertson), pp. 1–74.
619 Geological Society of London, Special Publication no. 17.
- 620 Sarkaya, A. R., Seyrek, T. 1976. YeŐilova- Tefenni Peridotit Masifindeki Krom ve Nikel ZenginleŐmeleri prospeksiyon
621 Raporu. MTA Rapor No: 5764, Ankara (unpublished).
- 622 Sarp, H. 1976. Etude Geologique et Petrographique du Corgege Ophiolitique de la Region Situee au Nord- Guest de Yesilova
623 (Burdur-Turguie), These, Univ. Ceneve, 378.
- 624 Őenel, M. 1991. Likya Napları iindeki volkanit katkılı Paleosen-Eosen okelleri: Faralya Formasyonu. Maden Tetkik ve
625 Arama Dergisi, 113, 1-14.
- 626 Őenel, M. 1997. 1:100.000 ölekli Türkiye Jeoloji Haritaları Isparta J9 (M23) paftası, MTA Yayın No: 16, Ankara.
- 627 Őenel, M., Akdeniz, N., Őztürk, E. M., Őzdemir, T., Kadıncık, G., Metin, Y., Öcal, H., Serdarođlu, M., Örcen, S. 1994.
628 Fethiye (Muđla)-Kalkan (Antalya) ve kuzeyinin jeolojisi, MTA Rapor No: 9761, Ankara (unpublished).

- 629 Şenel, M., Dalkılıç H., Gedik, İ., Serdaroğlu, M., Bölükbaşı, A.S., Metin, S., Esentürk, K., Bilgin, A.Z., Uğuz, M.F., Özgül,
630 N. 1992. Eğirdir-Yenişarbademli-Gebiz ve Geriş-Köprülü (Isparta-Antalya) Arasında Kalan Alanların Jeolojisi,
631 TPAO Rapor No: 3132, MTA Rapor No: 9390, Ankara (unpublished).
- 632 Şenel, M., Selçuk, H., Bilgin, Z. R., Şen, A. M., Karaman, T., Dinçer, M A., Durukan, E., Arbas, A., Örcen, S., Bilgi, C.
633 1989. Çameli (Denizli)-Yeşilova (Burdur)-Elmalı (Antalya) ve dolayının jeolojisi, MTA Rapor No: 9429, Ankara
634 (unpublished).
- 635 Şengör, A. M. C., Yılmaz, Y. 1981. Tethyan evolution of Turkey: A plate tectonic approach, *Tectonophysics*, 75, 181– 241.
- 636 Yağmurlu, F. 1991. Yalvac-Yarıkkaya Neojen havzasının tektonosedimanter özellikleri ve yapısal evrimi, *MTA Dergisi*,
637 112:1–13.
- 638 Yılmaz, Y. 1993. New evidence and model on the evolution of the southeast Anatolian Orogen. *Geological Society of*
639 *America Bulletin* 105, 251-271.